AN ASSESSMENT OF THE REPRODUCTIVE TOXICITY OF THE ANTI-COVID-19 DRUG MOLNUPIRAVIR USING STEM CELL-BASED EMBRYO MODELS

A MASTER'S THESIS SUBMITTED TO THE GRADUATE DIVISION OF THE UNIVERSITY OF HAWAI'I AT MĀNOA IN PARTIAL FULFILLMENT OF THE REQUIREMENTS FOR THE DEGREE OF

MASTER OF SCIENCE

IN

DEVELOPMENTAL AND REPRODUCTIVE BIOLOGY

MAY 2023

By

Margaret Carrell Huntsman

Thesis Committee:

Yusuke Marikawa, Chairperson

Yukiko Yamazaki

Vernadeth Alarcon

Acknowledgments

I would like to thank my thesis advisor, Dr. Yusuke Marikawa for his guidance and dedication to helping me throughout my research and thesis work. I would also like to thank my thesis committee members, Dr. Yukiko Yamazaki and Dr. Vernadeth Alarcon for dedicating their time and expertise to help me better my project. Finally, I would like to thank my family and friends for all their help and support.

Abstract

It is important that women of reproductive potential know what risks the medications they are consuming pose to reproductive health. However, reproductive risk information is particularly limited for new drugs, such as those to treat COVID-19. Because the FDA no longer requires *in vivo* animal testing during preclinical tests, the information obtained through suitable *in vitro* models are particularly crucial. The overall objective of this study was to evaluate the embryotoxic effects of molnupiravir, an anti-COVID-19 drug, using *in vitro* embryo models made of pluripotent stem cells. In Specific Aim 1, the efficacy of morphological assay using mouse P19C5 stem cell model, or embryoid bodies (EBs), was assessed in reference to known embryotoxic drugs. The ICH recently released a list of drugs with their *in vivo* concentrations known to cause embryotoxic effects. This ICH list can be used to validate the sensitivity and specificity of an *in vitro* assay to identify embryotoxicity. Adverse effects of drugs on the P19C5 EB model were determined from disruptions in morphology. The *in vitro* results with P19C5 EBs closely reflected those of the ICH's *in vivo* results for many of the drugs examined, validating the efficacy of the assay. In Specific Aim 2, the adverse effects of molnupiravir, and its metabolite N-hydroxycytidine (NHC) were examined using *in vitro* embryo models made of P19C5 cells and also of human embryonic stem cells. Morphology-based analyses indicated that molnupiravir had an adverse effect at concentrations much higher than the therapeutic level, whereas NHC had a dose-dependent adverse effects at therapeutically relevant concentrations. Molecular studies using P19C5 EBs further demonstrated that NHC altered the expression patterns of several embryo-patterning genes, providing mechanistic insights into the embryotoxic action of molnupiravir. These results emphasize the need for further studies into the effectiveness of the *in vitro* embryo models and the embryotoxic effects of the COVID-19 antiviral drugs.

Table of Contents

List of Tables

List of Figures

Chapter 1: Introduction

1.1 Teratogens

In the United States, more than 90% of women who are pregnant or breastfeeding take at least one medication (NICHD, 2022). Due to the sheer number of medications being consumed by those of reproductive potential it would follow that at least some of these medications could be dangerous to the fetus. Recent data suggest that over 1 in 16 pregnancies in the United States were exposed to teratogens in the past decade (Sarayani et al., 2022). Teratogens are "substances that may produce physical or functional defects in the human embryo or fetus after the pregnant woman is exposed" (Tantibanchachai, 2014). Teratogens can cause a wide variety of birth defects. In fact, the term teratogen was derived from the Greek word *teratos* which means monster (Tantibanchachai, 2014). Because of the dangerous effects of teratogens, it is incredibly important for women who are pregnant or about to become pregnant to be able to know if the medications they need to take are safe for embryos.

Prior to 2015, all drugs approved by the Food and Drug Administration (FDA) were sorted into five pregnancy risk categories, A, B, C, D and X (Drugs.com, 2023). This method was abandoned due to its over simplicity and potential for confusion, and was replaced with a new format in order to provide a more complex categorization of drugs from reproductive age to lactation. This new format, the Pregnancy and Lactation Labeling Final Rule, allows for more descriptive explanations of why a drug is considered harmful during three different stages, reproductive potential, pregnancy and lactation (Drugs.com, 2023). This is especially useful for drugs which may have a beneficial effect for the patient, such as essential medications for diabetes or cancer treatment. Some medications may be only harmful during certain stages such

as a particular trimester or during lactation. One famous example is the anti-emetic thalidomide which was widely prescribed to pregnant women in the 1950s (Vargesson, 2015). Some babies born to mothers taking this drug suffered limb defects and even death. However, these negative effects only occur if thalidomide is taken between 20 and 36 days post fertilization (dpf). Even though thalidomide is currently contraindicated for pregnancy it is nowadays used to treat a number of conditions, especially leprosy. Some drugs may carry the risk of harm, but these risks are outweighed by the beneficial effects of the medication. For a drug like thalidomide, many details need to be taken into account including the stage of embryonic development, the importance of the medication to the health of the mother, and any possible treatment alternatives that are available.

1.2 Assessment of Drug Safety for Reproduction

It is incredibly important for those who are pregnant or are planning to become pregnant to know that the medications they are taking have been thoroughly tested for reproductive safety. However, this is often not the case especially for newly released drugs like the ones marketed to treat COVID-19. New pharmaceuticals have to be approved through a lengthy multi-stage assessment process. Typically, it involves the initial discovery and development, then preclinical animal test, human clinical trials, drug review for approval to market and finally, post market-drug safety monitoring (FDA, 2018).

1.2.1 Preclinical Tests Using Animals

Preclinical research is the stage where toxicity is assessed by animal testing usually occurs, involving in a living organism. Tests are conducted in model organisms such as rats,

mice and rabbits. Rats and mice are good model species since they already have a lot of data about them published and they are more practical than other mammalian species for experimental purposes (EMA, 2020). Rabbits are another useful model organism for *in vivo* studies, while they can be a bit more unwieldy than rats or mice. However, rabbits can detect certain human teratogens that the former cannot, such as thalidomide. Importantly, no matter how good an animal model is, it will never be a 100% match to human biology. Thus, the need for the next step in the approval process is human clinical trials.

1.2.2 Human Clinical Trials

Once a drug has passed animal testing, it moves on to the third step of the drug development process the clinical trial. Clinical trials are divided into four phases. The first phase tests for safety and dosage, the second for efficacy and side effects, the third and fourth phase continue with close monitoring of adverse reactions and efficacy over larger and larger sample sizes (FDA, 2018). This process usually takes a few years to go through all the phases. Clinical trials have the unique ability to show the effects in the body when a drug is taken and allows harmful effects to be closely monitored by developers. Critically, pregnant women are almost always excluded from the trial process so it is difficult to predict how a medication will affect an embryo based solely on human clinical trials. After clinical trials are concluded, the FDA reviews the drug, if approved the drug is then "labeled" with proper prescribing directions by a joint effort between drug developers and the FDA (see 1.1) (FDA, 2018).

1.2.3 Post-Marketing Monitoring

The monitoring of adverse effects does not end after a drug has been approved. In certain cases, a pregnant woman may take a medication that is still in the trial process or has not been deemed safe for pregnancy. In these instances, the drug manufacturer will often set up a hotline or website where the pregnant woman and her physician can document their experience with the drug. There are also MedWatch where consumers or physicians can report problems with a medication directly to the FDA (FDA 2018). These sites are often the only way direct data can be collected on the effects of a drug on fetal development as it is ongoing.

1.2.4 Ethics of Animal Testing

There is controversy surrounding *in vivo* animal tests as many believe that they are unethical. While human clinical trials require informed consent, animals obviously cannot give consent and these trials are often painful or fatal. The issue of informed consent also appears in cases with human cells (see 1.4). The issues regarding animal suffering in research has been long known. In their 1959 book, *The Principles of Humane Experimental Technique* Russell and Burch, described the 3Rs for removing inhumanity in animal testing; Replacement, Reduction and Refinement. That is replacing animals with less counterparts of lesser consciousness, reducing the number of animals used in a study and refining methods to reduce harm. In December of 2022, the United States passed a new law that allows new medications to enter the human trial stage without the use of *in vivo* animal tests, provided that a suitable non-animal-based *in vitro* tests were completed in its stead (Wadman, 2023). These alternative tests can include a variety of assay types, including organoids, organ chips and stem-cell based *in vitro* embryo models.

1.3 Stem Cell-Based Models

In vitro embryo models can be made from pluripotent stem cells. Stem cells were first discovered in mice in 1963 as hematopoietic precursors. In 1980s, mouse embryonic stem cells (ESCs) were derived from blastocyst stage embryos, which possessed the pluripotency equivalent to the inner cell mass (ICM), the precursor of the entire fetal body. This is followed by the creation of the first human ESCs in 1998 (Piersma et al., 2022). There are many different classifications of stem cells, however they all share the ability to differentiate and self-renew in a laboratory setting. A stem cells classification represents its potential to turn into different cells. Namely, a totipotent stem cell can differentiate into any cell types including those derived from the trophectoderm, which becomes the placenta and ICM. A pluripotent stem cell can differentiate into any cell types derived from the ICM or any cell types in the body. ESCs which are generated from ICM, are pluripotent. There are also multipotent stem cells which are limited to cells within a particular germ layer, and unipotent stem cells which can only turn into one type of cell.

Stem cell models can mimic certain stages of early development *in vitro*. Pluripotent stem cell (PSC) testing has been used in predicative toxicology as an alternative to traditional *in vivo* animal testing (Piersma et al., 2022). There are many types of stem cell-based models for early development. Some models are made of induced pluripotent stem cells, iPSCs, while some are made from ESCs, for both mouse and humans.

Initially, mouse ESCs were used as a stem cell-based model for the embryotoxicity assessment of chemicals. Mice are considered a good model system for early human embryonic development for a number of reasons. They have similar embryological development to humans and the genetics are largely conserved between humans and mice (Moon, 2006). Later, human

ESCs were used to make *in vitro* embryo models that may be closer to human embryos. Furthermore, iPSCs, particularly of human, have been explored to circumvent potential ethical issues associated with the use of human ESCs, as the latter was originally generated by destroying human preimplantation embryos. Regardless of their nature and type, pluripotent stem cells play pivotal roles in creating *in vitro* embryo models for both basic research as well as embryotoxicity assessment (Piersma et al., 2022).

While there is variation in the types of stem cell that can be used, there is also variation in the different types of models and analyses that can be created with these cells. Specific organ systems or cell lines can be created; such as creating organoids of the liver or differentiating ESCs into cardiomyocytes. Cardiomyocyte differentiation is especially significant in a historical sense, as it was the first stem cell-based model to assess the embryotoxicity of chemicals. Another method is the creation of embryoid bodies (EBs). EBs are created by aggregation of pluripotent stem cells to mimic the cell-cell interactions and morphogenesis of a growing embryo (Piersma et al., 2022).

One of the assays utilizing the morphogenesis of EBs to detect embryotoxicity is the P19C5 EB model. The P19C5 EB model is derived from P19C5 mouse embryonal carcinoma cells which behave similarly to cells of the epiblast (Marikawa et al., 2009). These cells are not technically ESCs since they are derived from a teratoma rather than an ICM. The morphological changes that the P19C5 EBs undergo is similar to the posterior axial elongation that occurs in embryos during gastrulation (Marikawa et al., 2009). Thus, the elongation of cell aggregates can simulate axial patterning and elongation of early gastrulating embryos. The P19C5 EB model has been used to investigate developmental toxicity of a number of different drugs that are known embryotoxic chemicals *in vivo* (Li & Marikawa, 2016; Warkus & Marikawa, 2017).

Furthermore, the model has been shown to correctly model changes to key developmental pathways in a consistent manner with *in vivo* studies (Li and Marikawa, 2015).

Even though these stem cell models recapitulate only limited aspect of embryo development, they have many advantages. One advantage is that these models allow for the testing of chemical's metabolite individually. In many *in vivo* studies, it is only possible to study the effects of a drug as it is taken, instead of being able to study the effect of the drug during each step of the metabolism process. Another advantage is that process allows for the analysis of the particular molecular mechanism responsible for the drug's teratogenic effect. Which specific genes are impacted by a drug and during which stage of development, can be more effectively and precisely investigated, as *in vitro* models are amenable to various experimental analyses at the molecular levels. This allows for the study of precise dose/effect relationships; how a minor change in dosage can affect the overall development of the embryo, and also interrogation of molecular pathways that may be affected by chemical exposures.

1.4 History of Molnupiravir

New medications are often not thoroughly investigated for their impact on reproductive safety. This includes new medications to treat COVID-19 in response to the recent pandemic. One of these new drugs marketed is molnupiravir. Molnupiravir (EIDD-2801) is a prodrug of an active metabolite form EIDD-1931 also known as N-hydroxycytidine or NHC (Painter, 2020). NHC was discovered in 1961, by researchers at the University of Wisconsin who were investigating mutagens (Waters et al., 2022). It was then investigated for possible antiviral properties in 2004 but was found to be too mutagenic. Molnupiravir was then investigated by the Emory Institute for Drug Development (EIDD) to treat viruses such as Venezuelan equine

encephalitis in 2014 (Halford, 2020). These results showed promise, however, the interest in molnupiravir did not truly grow until the outbreak of COVID-19. Soon after the start of the pandemic, molnupiravir was acquired by Merck and Ridgeback Biotherapeutics for production on July 1, 2020 (Waters et al., 2022). Molnupiravir is a more accessible than the only FDA-approved COVID-19 drug remdesivir due to its oral availability. Molnupiravir is marketed under the brand name Lagevrio and it is currently authorized for emergency use in the United States, Japan, South Korea and China. It is still awaiting authorization use in the EU.

Molnupiravir is part of a class of antivirals called ribonucleoside analogues. Once in the cell, molnupiravir is rapidly metabolized into NHC triphosphate which acts on a virus' RNA-dependent RNA polymerase (RdRp) to incorporate itself into the viral genome, leading to a catastrophic mutation cascade (Hashemian et al., 2022; Urakova et al., 2018). However, some studies implicate a mutagenic activity of molnupiravir. One study found that NHC had the potential to cause harm to the host via incorporation into the host's genomic DNA, triggering mutagenesis (Zhou et al., 2021). Another study found mutations in nuclear and mitochondrial DNA in cells treated with 10μM of NHC for 3 days, but not enough mutation to disrupt mitochondrial function (Stitcher et al., 2020). Merck themselves reported animal studies, which have shown some teratogenic effects of molnupiravir. Namely, oral administration of molnupiravir to pregnant rats during the period of organogenesis caused embryo-fetal lethality and malformations of the eye, kidney, and axial skeleton (Merck 2023) above human NHC exposure levels (Blanchard, 2021). Currently, the mechanisms underlying the teratogenic action of molnupiravir are unknown.

1.5 Emergency Use Authorization

It is important to note that molnupiravir is authorized for emergency use only and it has not been fully approved by the FDA. The Emergency Use Authorization or EUA system was developed to allow the FDA to better respond to public health emergencies, be it a global pandemic or a biological attack (FDA 2023). An EUA allows a drug or device to bypass the usual, considerably lengthy, approval process. These can only be used when a public safety emergency is declared by the Secretary of the Department of Health and Human Services. This was the case for drugs and biologics relating to COVID-19 on March 27, 2020 (*Emergency Use*). When an EUA is issued, "the FDA must determine, among other things, that the product may be effective in diagnosing, treating, or preventing a serious or life-threatening disease or condition caused by a chemical, biological, radiological, or nuclear agent; that the known and potential benefits outweigh the known and potential risks for the product; and that there are no adequate, approved, and available alternatives" (FDA 2023). Thus, any drug released under an EUA must be met with more scrutiny than a fully approved pharmaceutical product. This is especially true, when it comes to reproductive toxicity since little to no tests for reproductive safety have been done in human when the authorization is given.

1.6 The Objective and Specific Aims of the Thesis Project

The objective of this thesis project is to utilize stem cell-based *in vitro* embryo models, particularly P19C5 EBs, to provide mechanistic insights into the embryotoxic action of molnupiravir. The following two Specific Aims are pursued.

Aim 1: *Test the sensitivity and specificity of the P19C5 embryoid body model to detect embryotoxicity of drugs*

The P19C5 EB model is made from pluripotent mouse stem cells which behave similarly to the epiblast (Marikawa et al., 2009). The efficiency of the P19C5 EB model to detect embryotoxic chemical exposures was validated in the previous studies in reference to various compounds with known *in vivo* embryotoxic concentrations (Li & Marikawa, 2016; Warkus & Marikawa, 2017). Nonetheless, further validation using additional compounds, particularly human medications would be beneficial in order to highlight the effectiveness of this model. Recently, the International Council for Harmonization of Technical Requirements for Pharmaceuticals for Human Use (ICH) released a guideline, which contains collection of known teratogens, specifically human medications and their *in vivo* maximum concentrations (C_{max}) in the plasma that are known to cause embryotoxic effects in rats, rabbits and/or human (EMA, 2020). The intention of this guideline, Detection of Reproductive and Developmental Toxicity for Human Pharmaceuticals Guidance for Industry, is to provide reference information to validate the sensitivity and specificity of alternative assays to detect embryotoxic drugs. Here, this ICH list of reference drugs is used to further validate the sensitivity and specificity of the P19C5 EB-based assay.

Aim 2: *Examine the embryotoxic effects of molnupiravir, anti-COVID-19 medication, using the stem cell-based embryo models*

The antiviral molnupiravir has been given Emergency Use Authorization by the FDA to treat COVID-19. It is important for those who are pregnant or who wish to become pregnant to know the effects that this medication may have on the embryo. This study looks at the effects of

molnupiravir and its metabolite NHC on embryo development using stem cell-based embryo models. Specifically, the study will determine the concentration-effect relationship for molnupiravir and NHC individually in relation to their therapeutic concentrations, and also examine the impact on the expressions of genes that regulate differentiation and patterning of early embryos. Such information should provide significant insights into the teratogenic action of molnupiravir and possibly help identify alternative anti-COVID-19 drugs that are safer for embryos.

Chapter 2: Materials and Methods

2.1 Test Drugs

All the drugs investigated in this study were commercially acquired. Namely, bosentan, busulfan, dabrafenib, ibrutinib, pazopanib, phenytoin, ribavirin, vismodegib, molnupiravir (EIDD-2801), and N-hydroxycytidine (NHC; EIDD-1931) are from Cayman Chemicals, while methotrexate, valproic acid, and cytidine were from Sigma-Aldrich. All drugs, except for valproic acid and cytidine, were dissolved in dimethyl sulfoxide (DMSO) as stocks and stored at -20°C. The stocks of valproic acid and cytidine were made in H_2O. Drugs were diluted to reach desired concentrations in the differentiation medium, containing the final concentration of 1% DMSO, immediately before experiments.

2.2 Cell Culture and Generation of Embryoid Bodies

P19C5 mouse embryonal carcinoma cells (Lau & Marikawa, 2014) were cultured in medium containing MEM alpha along with 7.5% Newborn Calf Serum, 2.5% Fetal Bovine Serum (FBS), and 50 U/mL penicillin and 50 μg/mL streptomycin (Life Technologies). These cells were passaged every other day. In order to generate embryoid bodies (EBs), the cells were aggregated in hanging drops, as previously described (Marikawa et al., 2009). Briefly, the cells were first dissociated in TrypLE Express and then suspended in the culture medium containing 1% DMSO with or without the desired concentration of the test drug, with a final density of 10 cells/μL. Sixteen drops of suspended cell solution (20 μL each) were placed on the interior of a lid of a 60 mm petri dish in a 4 x 4 pattern. The base of the petri dish was filled with 6 mL phosphate-buffered saline (PBS) and the lid was placed back on the petri dish. The dishes were

kept in an incubator at 37°C with 5% CO_2 and development was observed daily for 4 days. At day 4, EBs were collected for morphometric analysis or at daily for gene expression analysis.

Human embryonic stem cells (H9 line; WiCell Institute) were maintained in mTeSR1 culture medium (StemCell Technologies). To generate morphogenetic EBs, H9 cells were first dissociated with TrypLE Express and then aggregated in the differentiation medium, consisting of MEM alpha, 20% mTeSR1 5x supplement, 10 μM CHIR99021 (Wnt signaling activator), 2 μM SB431542 (Nodal signaling inhibitor), and 2 nM retinoic acid, according to the protocol reported previously (Marikawa et al., 2020). To test the effects of molnupiravir and NHC, desired concentrations of each drug were diluted in the differentiation medium prior to experiments.

2.3 Morphometric Analysis

Morphometric analysis was performed on the EBs to compare the effects of the different drugs of interest on their growth and elongation compared to the control. EBs were collected at day 4 for imaging using a Pasteur pipette and transferred into a petri dish with PBS. The EBs were gathered together within one frame for photography using gentle manipulation. Images were captured as JPEG files with an AxioCam MRm digital camera (Carl Zeiss, Thornwood, NY) attached to an Axiovert 200 inverted microscope with Hoffman modulation contrast optics (Carl Zeiss) and controlled by AxioVision software (Carl Zeiss). Once the images were collected, they were opened in ImageJ (http://imagej.nih.gov/ij/) as JPEG files for morphological analysis. Each EB was outlined using the polygon selection tool to determine their size and elongation. Size is indicated by area while elongation is indicated by Elongation Distortion Index (EDI) and Aspect Ratio (AR). EDI is calculated from the circularity value given by ImageJ using

the following formula EDI = [(1/Circularity) - 1]. For further analyses, AR was converted to adjusted AR, which equals AR-1. For EDI and adjusted AR (simply referred to as AR in this study hereafter), the values are zero for completely spherical EBs, while the value becomes higher when EBs are more elongated. Morphology data was collected for 14-16 EBs per set with 3 sets per drug concentration treatment, and thus 45-48 EBs per treatment group.

2.4 qRT-PCR

EB samples were harvested at day 0, 1, 2, 3 and 4 of culture for gene expression analysis. First the RNA was purified. The cells were lysed with 260 μL Trizol to allow access to the RNA. This sample was then used for RNA purification using the Direct-zol RNA MicroPrep kit (Zymo Research). This process utilized a spin column to purify total RNA from the sample lysed in the Trizol. The RNA was eluted from the column in 16 μL of RNAse free water. cDNA synthesis was conducted immediately following the purification of the RNA. This was done by adding 5 μL of 5X RT buffer, 2 μL of oligo dT primer, 1.5 μL dNTP mix, 0.5 μL of RNAse inhibitor and 1 μL of MMLV-RT (Promega) per sample (15 μL of RNA solution). This solution was then incubated for 1-3 hours at 42 °C and then 5 minutes at 90°C to deactivate the MMLV-RT before being quickly cooled in a cold block. The cDNA could then be used for quantitative Polymerase Chain Reaction (PCR). This was performed with SsoAdvanced Universal SYBR Green Supermix (Bio-Rad) using the CFX96 Real-Time System (Bio Rad). Six sets were analyzed using the samples from day 0-4. Ct values were collected and further analyzed using Microsoft Excel. *Actb* which encodes beta-Actin was used as the housekeeping gene for expression level normalization for the genes of interest. The characteristics of the genes investigated are listed in Table 1.

2.5 Statistical Analyses

Statistical analyses were performed using Microsoft Excel. Each P19C5 hanging drop culture for morphometric analysis was repeated three times, with the exception of the hanging drops for excess cytidine experiment (3.2.4) which was repeated four times. For consistency across sets, the morphological values (area, EDI, and AR) of individual EBs were normalized to an average value of the corresponding control EBs in each set. Thus, the data for each drug treatment group was represented as a relative value with control as 100%. The results of all sets were compiled and averaged together with a confidence interval of 95%. A two-sample t-test was performed to verify significant differences in area, EDI and AR between each treatment concentration and control. Statistical significance was determined to have a p-value of <0.01. When the values of drug treatment group were less than the control by >20% for EB growth (area) and/or different from the control by >40% for EB elongation (EDI or AR), the effect of drug treatment was deemed "adverse", according to the criteria established in the previous study (Warkus & Marikawa, 2017). Based on these morphometric criteria the No Observed Adverse Effect Level (NOAEL) was determined as the highest concentration level where a tested drug had no adverse effect on the model. The Lowest Observed Adverse Effect Level (LOAEL) was determined as the lowest concentration level where a tested drug showed an adverse effect on the model. The geometric mean between NOAEL and LOAEL was calculated as ($\sqrt{NOAEL*LOAEL}$) for comparison between *in vivo* and *in vitro* results. When the differences between the *in vitro* and *in vivo* geometrical means is less than 4-fold, it was deemed that the *in vitro* data is largely in line with the *in vivo* data.

For the initial gene expression study (time course analysis), six sets of EBs were harvested. Nine samples were collected per set, day 0 (dissociated cells prior to aggregation), 4 samples of control EBs (days 1-4 treated with DMSO only) and 4 samples of treated EBs (days 1-4 treated with 20 μM NHC). A second round of gene expression analysis (concentration-effect relationship) was conducted with five sets of EBs. Six samples were collected per set, control (0 μM NHC) and 5 dilutions (1.25, 2.5, 5, 10 and 20 NHC μM). Expression levels were normalized for each set and the average and standard deviation were calculated. A two-sample t-test was performed to verify significant differences between the treated groups and control. Statistical significance was determined to have a p-value of <0.05.

Chapter 3: Results

Specific Aim 1: Test the sensitivity and specificity of the P19C5 embryoid body model to detect embryotoxicity of drugs

3.1 Effects of drugs on the embryoid body morphology correlate with the data collected from *in vivo* embryotoxicity studies

To validate the effectiveness of the assay using P19C5 embryoid bodies (EBs) the effects of several known teratogens on the EB morphology were examined and compared to the *in vivo* embryotoxicity data in the ICH's guidance (EMA, 2020). This guidance provides the information on the maximum plasma concentration (C_{max}) of drugs in rats with respect to their reproductive outcomes. The information includes the lowest C_{max} associated with adverse outcomes (i.e., embryo loss or malformation) and the highest C_{max} associated with no adverse outcomes. The former is referred to the *in vivo* LOAEL) while the latter to the *in vivo* NOAEL. In this study, several drugs in the ICH list were examined using the P19C5 EB-based assay, and their *in vitro* adverse effects concentrations were compared with the in vivo LOAEL and NOAEL.

Ten drugs from the ICH list were selected, which include a wide range of teratogen types; They are bosentan, busulfan, dabrafenib, ibrutinib, methotrexate, pazopanib, phenytoin, ribavirin, valproic acid, and vismodegib. Each drug was then tested using the EB morphology assay. The cell aggregates were cultured in hanging drops of medium, containing varying concentrations of the drug for four days, at which point the EBs were imaged. They were then measured for three morphological parameters: one parameter (area) for growth; and two (EDI and AR) for elongation (see Materials and Methods for details). An effect was deemed "adverse"

when it caused a >20% reduction in area and/or a >40% change in EDI or AR, according to the criteria reported previously (Warkus & Marikawa 2017). *In vitro* NOAEL and LOAEL were established from these adverse effect levels. The *in vitro* NOAEL and LOAEL or their geometrical mean were then compared with the *in vivo* NOAEL and LOAEL reported in the ICH list (see Materials and Methods). Of these drugs, the *in vitro* effects of seven drugs (bosentan, dabrafenib, ibrutinib, methotrexate, phenytoin, valproic acid and vismodegib) were largely in line with *in vivo* data, whereas those of the other three drugs (busulfan, pazopanib and ribavirin) appeared different from those of the *in vivo* data. The results of individual test drugs are described below.

3.1.1 Bosentan

Bosentan is a medication used to treat pulmonary artery hypertension and is an endothelin 1 antagonist (Masarweh & Bhardwaj, 2023). By preventing endothelin from binding to endothelin A and endothelin B receptors, bosentan causes a reduction in vasoconstriction and bronchoconstriction respectively. In rat embryotoxicity studies, bosentan was found to cause agenesis of the soft palate and skull abnormalities in the fetus (EMA, 2020). In the P19C5 EB assay bosentan exhibited adverse effects at 16 μM and higher (Fig. 1). At these concentrations bosentan treatment caused less growth in EB as shown by reduced area. Bosentan also diminished elongation as shown by significantly reduced EDI and AR at 32 μM and higher. The geometric mean of *in vitro* NOAEL and LOAEL was 11.3 μM. By contrast the *in vivo* NOAEL and LOAEL were 8.16 μM and 29.46 μM respectively with a geometric mean of 15.5 μM. Thus, the P19C5 EB assay result is largely in line with *in vivo* data, as the difference between the *in*

vivo and *in vitro* means (i.e., 15.5/11/3= 1.37) is less than 4-fold (see Materials and Methods for the criteria).

3.1.2 Busulfan

Busulfan is a medication used to treat chronic myelogenous leukemia and is an alkylating agent (Busulfan). Busulfan replaces a hydrogen group on a cancer's DNA molecule with an alkyl group leading to inhibition of transcription. In rat embryotoxicity studies, busulfan was found to cause limb and rib malformations (EMA, 2020). In the P19C5 EB assay busulfan exhibited adverse effects at 40 μM and higher (Fig. 1). At these concentrations busulfan treatment caused less growth and elongation in EBs as shown by significantly reduced area, EDI and AR. No adverse effect was observed for busulfan at 20 μM. By contrast, the *in vivo* LOAEL of busulfan is 3.41 μM with no data available for NOAEL. Thus, it appears that the P19C5 EB model is less sensitive to the embryotoxicity of busulfan compared to *in vivo* because the *in vitro* LOAEL (40 μM) was much higher (> 4-fold) than the *in vivo* LOAEL (3.41 μM).

3.1.3 Dabrafenib

Dabrafenib is a medication used to treat malignant melanoma and is a bioactive inhibitor of the BRAF protein. By inhibiting the BRAF protein, dabrafenib works to prohibit tumor proliferation through the MAP kinase/ERKs signaling pathway (NCBI, Dabrafenib). In rat embryotoxicity studies, dabrafenib causes cardiac defects and decreases implantation (EMA, 2020). In the P19C5 EB assay dabrafenib showed adverse effects at 4 μM and higher (Fig. 1). At these concentrations dabrafenib caused less growth as shown by a decrease in area. The geometric mean of the *in vitro* NOAEL and LOAEL was 2.82 μM. By contrast the *in vivo*

NOAEL and LOAEL were 2.25 μM and 4.18 μM respectively, with a geometric mean of 3.07 μM. Thus, the P19C5 EB assay result is largely in line with *in vivo* data as the difference between the two means (3.07/2.83= 1.08) is less than 4-fold.

3.1.4 Ibrutinib

Ibrutinib is a medication used to treat refractory chronic lymphocytic leukemia and mantle cell lymphoma and is a Bruton's Tyrosine Kinase (BTK) inhibitor (NCBI, Ibrutinib). By inhibiting BTK, ibrutinib leads to a decrease in B-cell receptor signaling associated with overexpressed B-cell maturation in B-cell malignancies. In rats, ibrutinib causes cardiac malformations and increases post-implantation embryo loss (EMA, 2020). In the P19C5 EB assay, ibrutinib showed adverse effects at 8 μM and higher (Fig. 1). At these concentrations ibrutinib caused less growth as shown by a decrease in area and changes in elongation as shown by an elevated EDI and a significantly decreased AR. The geometric mean for the *in vitro* NOAEL and LOAEL was 5.66 μM. By contrast the *in vivo* NOAEL and LOAEL were 2.97 μM and 5.96 μM with a geometric mean of 4.21 μM. The difference between the *in vivo* and *in vitro* means (5.66/4.21=1.34) was less than 4-fold. Thus, the sensitivity of the P19C5 EB assay is comparable to *in vivo*.

3.1.5 Methotrexate

Methotrexate is a medication used to treat a variety or cancers, inflammatory and immune conditions and is a folic acid antagonist (Hannoodee & Mittal, 2023). By inhibiting the enzyme dihydrofolate reductase, methotrexate prevents the formation of the active form of folic acid therefore inhibiting nucleotide synthesis. In rat studies, methotrexate leads to fetal malformations

and litter reabsorption (EMA, 2020). In the P19C5 EB assay, methotrexate showed adverse effects at 0.04 μM and higher (Fig. 1). At these concentrations, methotrexate caused reduction in growth and elongation shown by decreases in area, EDI and AR. The *in vivo* LOAEL was 0.46 μM while NOAEL data is unavailable. Thus, the P19C5 EB assay was able to detect the embryotoxicity of methotrexate sensitively. However, because *in vivo* NOAEL data is lacking, it is unclear whether the *in vitro* assay is too sensitive to methotrexate.

3.1.6 Pazopanib

Pazopanib is a medication used to treat renal cell carcinoma and soft tissue sarcomas and is a multi-kinase inhibitor (NCBI, Pazopanib). By inhibiting various growth factor receptors, pazopanib leads to a decrease of angiogenesis in tumors. In rats, pazopanib administration leads to malformation in development of great vessels of the heart (EMA, 2020). In the P19C5 EB assay, pazopanib showed adverse effects at 1 μM and higher (Fig. 1). At 1 μM pazopanib caused a skinny appearance in EBs, causing an increase in EDI. At 4 μM of pazopanib, however, there was a reduction in both growth and elongation as shown by decreases in area, EDI and AR. The geometric mean for the *in vitro* NOAEL and LOAEL was 0.71 μM. By contrast the *in vivo* NOAEL and LOAEL in rat studies were 7.93 μM and 23.78 μM with a geometric mean of 13.73 μM. Thus, the P19C5 EB assay (mean = 0.71 μM) appears to be excessively more sensitive to pazopanib than *in vivo* (mean = 13.73 μM). Note, however, that the ICH guidance also provides the information on *in vivo* studies using rabbits, in which NOAEL and LOAEL are 0.30 μM and 2.43 μM, respectively. In this case, the *in vivo* geometrical mean (rabbit) is 0.85 μM, which is much closer to that of the P19C5 EB assay result.

3.1.7 Phenytoin

Phenytoin is a medication used to treat epilepsy and is a hydantoin derivative (Gupta & Tripp, 2023). By blocking voltage-dependent membrane sodium channels, phenytoin obstructs the positive feedback loop associated with focal seizures. In rats, phenytoin causes cranial and skeletal malformations (EMA, 2020). In the P19C5 EB assay, phenytoin showed adverse effects at 100 μM and higher (Fig. 1). At these concentrations, phenytoin caused a reduction in growth shown by a decrease in area. The geometric mean for the *in vitro* NOAEL and LOAEL was 70.71 μM. By contrast the *in vivo* NOAEL and LOAEL were 53.12 μM and 106.24 μM respectively with a geometric mean of 75.12 μM. Thus, as the difference between the two means (75.12/70.71=1.06) is very small the P19C5 EB assay result is highly reflective of the *in vivo* data.

3.1.8 Ribavirin

Ribavirin is an antiviral used to treat flavivirus infections including chronic hepatitis C and it is a nucleoside analogue (NCBI, Ribavirin). By acting as a guanosine analogue, ribavirin inhibits the function of RNA-dependent RNA polymerase impacting viral replication. In rats, ribavirin caused mutations throughout the fetus as well as an increase in post-implantation embryo loss (EMA, 2020). In the P19C5 EB assay, ribavirin showed adverse effects at 16 μM (Fig. 1). At this concentration, both growth and elongation were reduced as shown by decreases in area and AR. The geometric mean for the *in vitro* NOAEL and LOAEL was 11.31 μM. By contrast the *in vivo* NOAEL and LOAEL were 0.02 μM and 0.05 μM respectively with a geometric mean of 0.03μM. Thus, as the *in vitro* mean (11.3 μM) is much higher than the *in vivo*

mean (0.03 μM), it appears that the P19C5 EB assay is unable to detect the embryotoxicity of ribavirin in a sensitive manner.

3.1.9 Valproic acid

Valproic acid is a medication used to treat seizures and psychiatric conditions (Orney, 2009). It has a variety of functions, namely, blocking voltage gated channels, inhibiting histone deacetylase and increasing GABA concentrations in the central nervous system. In rats, valproic acid exposure led to neural and cardiovascular defects (EMA, 2020). In P19C5 EB assay valproic acid showed adverse effects at 400 μM and higher (Fig. 1). At these concentrations elongation was decreased as shown by a reduction in EDI. The geometric mean for the *in vitro* NOAEL and LOAEL was 282.84 μM. By contrast the *in vivo* NOAEL and LOAEL were 507.59 μM and 1574.08 μM respectively with a geometric mean of 893.86 μM. The difference between the two means (893.86/282.84=3.16) is less than 4-fold and thus, the P19C5 EB assay results are largely in line with the *in vivo* data.

3.1.10 Vismodegib

Vismodegib is a medication used to treat basal cell carcinoma (Zito et al., 2023). It blocks tumor mediating genes via the sonic hedgehog signaling by inhibition of the protein SMO. In rat studies, vismodegib exposure leads to craniofacial, limb and digit defects (EMA, 2020). In the P19C5 EB assay vismodegib showed adverse effects at 20 μM and higher (Fig. 1). At these concentrations, elongation was decreased as shown by a reduction in EDI and AR. The *in vivo* LOAEL was 17.14 μM with no NOAEL value reported. Thus, the P19C5 EB affected by vismodegib at a concentration that is close to the adverse level *in vivo.*

The *in vitro* data of all 10 test drugs in comparison with the ICH *in vivo* data are summarized in Table 2.

Specific Aim 2: Examine the embryotoxic effects of molnupiravir, anti-COVID-19 medication, using stem cell-based embryo models

3.2 Molnupiravir and its metabolite NHC significantly affect the development of embryoid bodies

The antiviral molnupiravir has been authorized by the FDA for emergency use for the treatment of COVID-19. After oral intake, molnupiravir enters the circulation, in which it is converted into NHC, acting as an active metabolite to cause mutations on the viral genome. To assess the embryotoxic potential of molnupiravir, mouse P19C5 cell aggregates or embryoid bodies (EBs) were cultured in different concentrations of molnupiravir and also its metabolite NHC and then analyzed for changes in EB morphology and gene expression.

3.2.1 Molnupiravir has an effect on the growth and elongation of the embryoid bodies

P19C5 EBs were cultured in different concentrations of molnupiravir for four days (0, 10, 20, 40, 80 μM) and then assessed for changes in morphology. Among these concentrations tested, only 80 μM significantly affected the EB morphology. Specifically, the area had decreased by 19.6%, the EDI had decreased by 35.1% and the AR had decreased by 30.6% (Fig. 2). Note that 80 μM is extremely higher than the plasma concentration of molnupiravir (<1 μM) found in people who received a therapeutic dose of molnupiravir (Painter et al., 2021).

3.2.2 NHC has an effect on the growth and elongation of the embryoid bodies at therapeutically relevant concentrations

P19C5 EBs were cultured in different concentrations of NHC for four days (0, 5, 10, 20, 40 μM) and then assessed for changes in morphology. At a concentration of 10 μM both growth (area) and elongation (EDI and AR) were significantly decreased from the control: the area had decreased by 13.3%, the EDI by 24.3% and the AR by 20.1%. There was an even greater extent of decrease at 20 μM where the area had decreased by 32.9%, the EDI by 69.7%, and AR 75.8% (Fig. 2). Note that the plasma concentration of NHC found in molnupiravir-administered people are 9.0-11.5 μM (Painter et al., 2021), indicating that NHC impairs the EB morphology at therapeutically relevant concentrations.

3.2.3 Gene expression patterns of developmental regulators are altered by NHC

To assess the nature of abnormalities caused by NHC at the molecular level, the gene expression profiles of NHC-treated EBs were examined. Here, EBs were cultured in 20 μM NHC for four days. This specific concentration was selected for analyses since it was the lowest level of concentration that exhibited "adverse" effect (i.e., area reduction by >20%), according to the previously established criteria (Warkus & Marikawa, 2017). On each day of culture a control (DMSO only) and a NHC sample were taken for RNA extraction followed by qRT-PCR analyses of developmental regulator genes. The expression levels of 15 different genes were analyzed over the course of the four days of culture. These 15 genes included pluripotency maintenance factors (*pou5f1*), primitive streak formation and mesoderm patterning (*brach, fgf8, foxc2, wnt3*), axial patterning (*cdx1, hoxa1, hoxb7, hoxc6, tbx6, wnt3a, wnt3*), and somite segmentation (*meox1, mesp2, aldh1a2, cyp26a1*). The molecular and functional properties of these genes are

summarized in Table 1. No significant change in expression was found for *pou5f1, wnt3a, wnt3, cyp26a1, mesp2, fgf8, hoxc6, hoxb7*, or *hoxa1* (Fig. 3). On day 1 of culture *tbx6* expression was decreased (Fig 3). On day 2 of culture, *aldh1a2* and tbx6 expression were decreased while *cdx1* expression was increased. On day 3 of culture, *foxc2, meox1* and *aldh1a2* expression were decreased while *tbx6* and *brach* were increased. On day 4, *foxc2, meox1* and *aldh1a2* expression were decreased.

There were a great deal of significant changes in expression level occurring on day 3 of culture, as described above. To further investigate the impact of NHC on these genes, the expression of the five genes affected, namely *aldh1a2, tbx6, foxc2, meox1* and *brach,* was measured at day 3 after being cultured in different concentrations of NHC (1.25, 2.5, 5, 10, 20 μM). The expression of aldh1a2 was increased at NHC concentrations of 1.25, 2.5, 5 μM and decreased at NHC concentration of 20 μM (Fig. 4). *Brach* did not show any significant changes in expression (Fig. 4). The expression of *tbx6* was decreased at 2.5 and 5 μM and significantly increased at 20 μM (Fig. 4). The expression of *foxc2* was significantly increased at NHC concentrations of 1.25, 2.5, 5 μM and significantly decreased at NHC concentration of 20 μM (Fig. 4). The expression of meox1 was significantly decreased at 10 and 20 μM. These results indicate that NHC alters gene expression patterns of developmental regulator genes even at the concentrations that did not significantly affect the EB morphology.

3.2.4 Excess amounts of cytidine block negative effects of NHC

NHC resembles cytidine nucleoside in chemical structure (Fig. 5) and takes its place during viral replication to cause lethal mutagenesis. It is possible that NHC cause abnormalities in P19C5 EBs also by acting as a cytidine-mimetic. To test whether this is the case, EBs were

exposed to an overabundance of cytidine nucleoside along with NHC, expecting that excess cytidine blocks the negative effects of NHC through competition. When exposed to an excess cytidine nucleoside (205 μM) and 20 μM of NHC, the extent of reduction in area (18.44%) was significantly less as compared to when exposed only to NHC (42.96%) (Fig. 5). Furthermore, EDI and AR were not affected when EBs were treated with NHC with excess cytidine, while NHC alone decreased these parameters by 50.73% and 48.19% respectively. Thus, excess cytidine significantly mitigated the negative effects of NHC.

3.2.5 NHC but not molnupiravir impairs the morphology of human stem cell model

The above studies using P19C5 EBs suggest that NHC, active metabolite of molnupiravir, impairs embryo development at therapeutically relevant concentrations, which is in line with preclinical animal studies by the pharmaceutical company (Merck, 2023). To date, however, no information is available whether molnupiravir or NHC also impairs human embryos. To gain further insight, here the morphogenesis model made of human embryonic stem cells (ESCs) was explored (Marikawa, et al., 2020). In this model, aggregates of human ESCs grow in size and elongate in shape as embryoid bodies (EBs) over the course of 5 days of culture in the presence of specific signaling modulators. Human ESC aggregates were exposed to varying concentration (1.25, 2.5, 5, 10, 20 μM) of molnupiravir and NHC for 5 days, followed by the measurement of morphological parameters, area, EDI and AR.

Molnupiravir exposure decreased elongation of human EBs at 5 μM and 10 μM (Fig. 6). There was a significantly reduced AR at 5 μM (48.1%) and a significantly reduced EDI at 10 μM (40.44%). However, the growth of EBs was not significantly reduced at any concentrations of molnupiravir tested. By contrast, NHC-exposed human EBs had markedly decreased elongation

in both EDI and AR at 5 μM (by 67% and 62.9% respectively), at 10 μM (81.5% and 77.5%) and at 20 μM (81.51% and 74.4%). Growth was also significantly reduced in the 20 μM concentration by 68.8%. These results suggest that the sensitivity of human morphogenesis model to molnupiravir and NHC is similar to that of the mouse P19C5 model, such that NHC, but not molnupiravir, impairs the growth and elongation at therapeutically relevant concentrations.

Chapter 4: Discussion

4.1 In vitro assay for teratogens using pluripotent stem cell-based embryo models

The goal of Specific Aim 1 was to examine the efficacy of the P19C5 EB model to assess developmental toxicity of chemicals based on the ICH report. The ICH report provides a collection of *in vivo* embryotoxicity levels of a number of known drugs in rats, rabbits and humans. The purpose of the ICH report is to provide a guideline to help validate the effectiveness of alternative assays, including stem cell-based *in vitro* systems, to detect embryotoxic drugs in a sensitive and specific manner. Thus far, according our review of literature, no assay system has been validated using the ICH chemical list. This thesis study aims to apply the ICH guideline to further validate the applicability of the P19C5 EB model for studying embryotoxicity. Although only ten of the 32 drugs provided in the ICH list were examined in this study, the analyses for the other drugs are currently ongoing.

Of the ten teratogens examined in this study, seven of them had *in vitro* results largely in line of the *in vivo* data. These seven were bosentan, dabrafenib, ibrutinib, methotrexate, phenytoin, valproic acid and vismodegib. The three teratogens that did not correlate were busulfan, pazopanib and ribavirin. Busulfan exposure to pregnant rats leads to carpal bone fusion in fetuses at the LOAEL (EMA, 2020). Since carpal development does not occur until just before parturition in rats (DeSesso and Scialli, 2018), it is possible that the negative effects of busulfan are not picked by the P19C5 EB assay, which mainly represents embryos at the gastrulation stage. Higher doses of busulfan in pregnant rats, lead to limb and rib malformations which occur much earlier in development making it more likely for their adverse effects to be detected by the P19C5 model.

Pazopanib inhibits vascular endothelial growth factor (VEGF) receptors. In pregnant rats, pazopanib exposure leads to malformations of the great vessels of the heart (EMA, 2020). Although the P19C5 EB assay appeared over-sensitive to pazopanib in comparison to the rat *in vivo* data, it was more in line with the rabbit *in vivo* data. In rabbits, pazopanib leads to increased post-implantation loss (EMA, 2020). Although the causes of such inter-species differences are currently unknown, the response of P19C5 EB to pazopanib may be more reflective of the events in rabbits that are sensitively impaired by pazopanib than rats. Further investigations into the molecular mechanisms underlying the adverse effects of pazopanib on P19C5 EBs (e.g., gene expression profiling) may shed light on how the drug impairs embryo development and how its sensitivity is different between species.

Ribavirin is another drug that appeared to be undetectable by the P19C5 EB assay in a sensitive manner. Here, metabolism may play a role, which is another important aspect to consider when interpreting *in vitro* test results. Some medications must be metabolized in the body to form an active metabolite in order to be effective. In an *in vivo* study this metabolite would be accounted for through the body's natural absorption of the medication. In the case of *in vivo* embryotoxicity studies, administered drugs may first be metabolized by the pregnant mother, and their metabolites reach developing embryos to cause abnormalities. In *in vitro* studies, on the other hand, there is no maternal system to metabolize drugs, so that individual metabolite may need to be studied. Ribavirin is known to be metabolized rapidly in the body into multiple metabolites, and it is currently unknown how much of an effect each of these metabolites has on embryo development (EMA, 2020). It may be important in future studies to examine individual metabolites of ribavirin using the P19C5 EB model, which may reveal whether the embryotoxicity of the drug is mediated through specific metabolites. Such

metabolite-specific investigations are not possible *in vivo* but are doable with *in vitro* models, where there is no maternal metabolism. In that sense, the lack of maternal metabolism in *in vitro* assays may be regarded as an advantage rather than a disadvantage.

In addition to embryo-derived pluripotent stem cells, such as ESCs and P19C5 cells, induced pluripotent stem cells (iPSCs) have been actively explored as *in vitro* models for teratogen assays (Piersma et al., 2022). Since they are made from adult cells, iPSCs, particularly of humans, do not have the same ethical drawbacks that hESCs suffer from. However, the use of iPSCs so far has been limited in part due to their tendency to retain some of the attributes of their lineage as a result of incomplete reprogramming of DNA methylation (Piersma et al., 2022). This retaining of their former lineage can make iPSCs difficult to fully program into an embryo-like model. Meanwhile, hESC-based assays are limited by ethical and governmental restrictions but can provide invaluable insight into the inner workings of early embryo development. Often, human embryological research is marred by ethical concerns that make finding the necessary funding and materials difficult. Many raise concerns about the destruction of human embryos required to make hESCs as well as what should be the proper methods for informed donation and consent (Lo & Parham, 2009). In the United States, under the 1995 Dickey-Wicker Amendment, federal funds cannot be used for research where a human embryo is created or destroyed (Kearl, 2010). This means that federal funds cannot be used to create new hESC lines which greatly limits the number of available cell lines for use. However, hESCs may be far more sensitive to post-gastrulation teratogenic effects and they eliminate the inter-species false negatives that can occur with mouse ESCs (Piersma et al., 2022).

As far as stem cell-based embryo models go, each model has its own strengths and weaknesses. For example, the harmful effects of some teratogens do not appear in mice as they

do in humans, one example being thalidomide. Furthermore, the P19C5 model focuses on gastrulation, so a teratogenic effect that occurs later in development may not be caught by this model. To get a better understanding of the effect of teratogens on embryo development it is necessary to employ multiple assay and model types. Further strengths and weaknesses of these models can be investigated using the reference chemical list provided by the ICH report.

4.2 Effects of molnupiravir on embryos

Molnupiravir and its metabolite NHC both affected the morphology of the P19C5 EBs in a dose dependent manner. Molnupiravir significantly affected the EB morphology at 80 μM while NHC did at much lower concentrations even at 10 μM (see 3.2). The therapeutically relevant concentrations for molnupiravir and NHC are <1 μM and 9.0-11.5 μM, respectively (Painter et al., 2021) which makes the effects of NHC more clinically relevant than molnupiravir itself. The morphological effects of molnupiravir and NHC were also dose-dependent in the human ESC-based assay with the sensitivity similar to P19C5 EBs. However, the molecular mechanisms underlying the effects of NHC still need to be analyzed for the human model.

In vivo concentration is based on C_{max} levels or the highest peak reported in plasma. As the drug in the plasma dissipates due to half-life (as a result of metabolism and excretion), *in vivo* concentration levels are not held constant at the C_{max} level. In the case of NHC, the half-life ranges from 3 to 6 hours (Hashemian et al., 2022). Additionally, NHC has been shown to not accumulate in plasma in human studies (Painter et al., 2021). In the P19C5 EB model, the concentration of drugs added to the culture medium is possibly constant throughout the 4 days of hanging drop culture, because there is no metabolism or excretion *in vitro*. This situation raises a concern that the *in vitro* situation may not be reflecting the physiological condition, where the

drug concentrations change over time. Further studies are necessary to determine what the effect of constant vs transient exposure levels has on the outcome of EB development. Furthermore, plasma concentration levels in a person treated with molnupiravir may also change depending on physiological factors of the patient such as kidney or liver dysfunction, which generally lower the excretion and metabolism respectively and increase drug concentrations as a result. Such circumstances may need to be taken into account when interpreting the experimental results and applying to clinical scenarios.

Exposure to NHC significantly downregulated the expression of key somite regulating genes *meox1* and *aldh1a2*. *Aldh1a2* encodes alcohol dehydrogenase which is necessary for the generation of retinoic acid (RA) from retinol. *Aldh1a2* knockout mice suffer from a number of embryological defects including shortening of anterior posterior axis, lack of limb development, heart malformation and death (Niederreither et al., 1999). *Meox1* is one of the genes responsible for somite segmentation. *Meox1* knockout mice suffer from mild defects to the axial skeleton, while a loss of both *meox1 and meox2* leads to a near complete loss of axial skeleton formation and its associated muscles (Mankoo et al., 2003). Future studies should investigate the effects of NHC on *meox2* expression. If *meox2* is as strongly downregulated as *meox1* it would aid in explaining the severe morphological effects observed in the NHC-exposed embryos.

Exposure to NHC upregulated the expression of *cdx1* on day 2 of culture and *brach* on day 3 of culture (see 3.2.3). *Cdx1* is important in establishing presomitic mesodermal fate and induces *brach* expression (Gouti et al., 2017). Therefore, an increase in *cdx1* expression on day 2 could lead to an increase in *brach* expression on day 3 of culture. The posterior of the embryo is full of bipotential precursors known as neuromesodermal progenitors (NMPs). The regulation of these NMPs is responsible for axial elongation in the embryo. RA signaling is initially required

to form NMPs and is then used to promote a neural fate. However, in the NHC exposed embryos, RA signaling may be depleted as implicated by the down regulation of *aldh1a2*. This means that the NMPs may be unable to adopt a neural fate and are instead be more inclined to become mesoderm. This is supported by the peak of *tbx6* expression occurring on day 3 rather than day 2 in NHC-treated EBs. *Tbx6* is a mesoderm-inducing factor that operates in adversity to *sox2* in an RA-controlled feedback loop (Gouti et al., 2017). Since, RA signaling is downregulated it is possible that there is a delay in NMP production leading to a later *tbx6* peak. Additionally, instead of increasing levels of *tbx6* leading to more RA signaling and inducing a neural fate, as would normally occur due to the feedback loop, *aldh1a2* expression remains decreased. Furthermore, *foxc2* expression which normally peaks on day 3 of culture, was significantly decreased. *Foxc2* is another important factor for sclerotome derived tissues, such as ribs and vertebrae (Winnier et al., 1997).

Why exactly NHC causes these effects are not entirely clear. A leading theory for the cytotoxicity caused by NHC is that of many ribonucleoside analogues. What makes them effective in fighting viruses like COVID-19 is their ability to be incorporated into the viral genome. However, during that process there is a point where NHC could be incorporated into the DNA of the host instead of the virus's RdRp. This process is most vulnerable in dividing cells where there is DNA precursors synthesis actively occurring (Zhou et al., 2021), places like a growing embryo. More research will need to be done to study how exactly NHC interacts with the DNA of the host and to what extent this interaction goes.

4.3 Concluding Remarks

As more and more people of reproductive potential are taking medication it is more important than ever that there are better methods for testing reproductive safety of drugs in a swift but effective manner. One method of testing cannot cover all aspects of embryo development; therefore, a multitude of complimentary studies are needed to provide the best possible view of a drug's embryotoxicity. As the FDA moves away from *in vivo* animal testing, more *in vitro* methods are coming into the spotlight. Pluripotent stem cell-based embryo models are a promising contributor to this collaboration. Although more work needs to be done to determine the full potential and limitations, with a relatively easy upkeep and high reproducibility, the P19C5 EB model and other stem-cell based assays are great alternatives to more traditional *in vivo* methods.

Table 1: Genes analyzed in P19C5 EBs in this study

Gene	Description
Actb	Cytoskeleton Actin, housekeeping gene, highly conserved.
Aldh1a2	Alcohol Dehydrogenase, retinoic acid (RA) signaling, somite segmentation
Brach (Brachyury)	T-box transcription factor T, primitive streak formation
Cdx1	Caudal Type Homeobox 1, axial patterning, induces posterior fate (Gouti et al., 2017)
Cyp26a1	Cytochrome P450 family subfamily A member 1, Encodes RA metabolizing enzyme, preventing RA signaling (Gouti et al., 2017)
Fgf8	Fibroblast growth factor 8, mesoderm patterning and primitive streak formation
Foxc2	Forkhead box protein C2, mesoderm patterning and primitive streak formation
Hoxa1	Homeobox A1, axial patterning
Hoxb7	Homeobox B7, axial patterning
Hoxc6	Homeobox C6, axial patterning
Meox1	Mesenchyme homeobox 1, axial patterning and somite segmentation (Mankoo et al., 2003)
Mesp2	Mesoderm posterior BHLH transcription factor 2, somite segmentation
Pou5f1	POU class 5 Homeobox 1 (OCT4), pluripotency maintenance
Tbx6	T-box transcription factor 6, axial patterning, promotes mesodermal fate (Gouti et al., 2017)
Wnt3	Wnt family member 3, primitive streak formation
Wnt3a	Wnt family member 3a, axial patterning, promotes mesodermal fate (Gouti et al., 2017)

Primer sequences previously described (Warkus and Marikawa., 2017)

Table 2: Effect levels in P19C5 EB assay and ICH report

	P19C5			ICH (rat)		
Drug Name	NOAEL (μM)	LOAEL (μM)	Geometric Mean(μM)	NOAEL (μM)	LOAEL (μM)	Geometric Mean(μM)
Bosentan	8	16	11.31	8.16	29.46	15.50
Busulfan	20	40	28.28	n/a	3.41	n/a
Dabrafenib	2	4	2.83	2.25	4.18	3.07
Ibrutinib	4	8	5.66	2.97	5.96	4.21
Methotrexate	0.02	0.04	0.03	n/a	0.46	n/a
Pazopanib	0.5	1	0.71	7.93	23.78	13.73
Phenytoin	50	100	70.71	53.12	106.24	75.12
Ribavirin	8	16	11.31	0.016	0.052	0.03
Valproic Acid	200	400	282.84	507.59	1574.08	893.86
Vismodegib	10	20	14.14	n/a	17.14	n/a

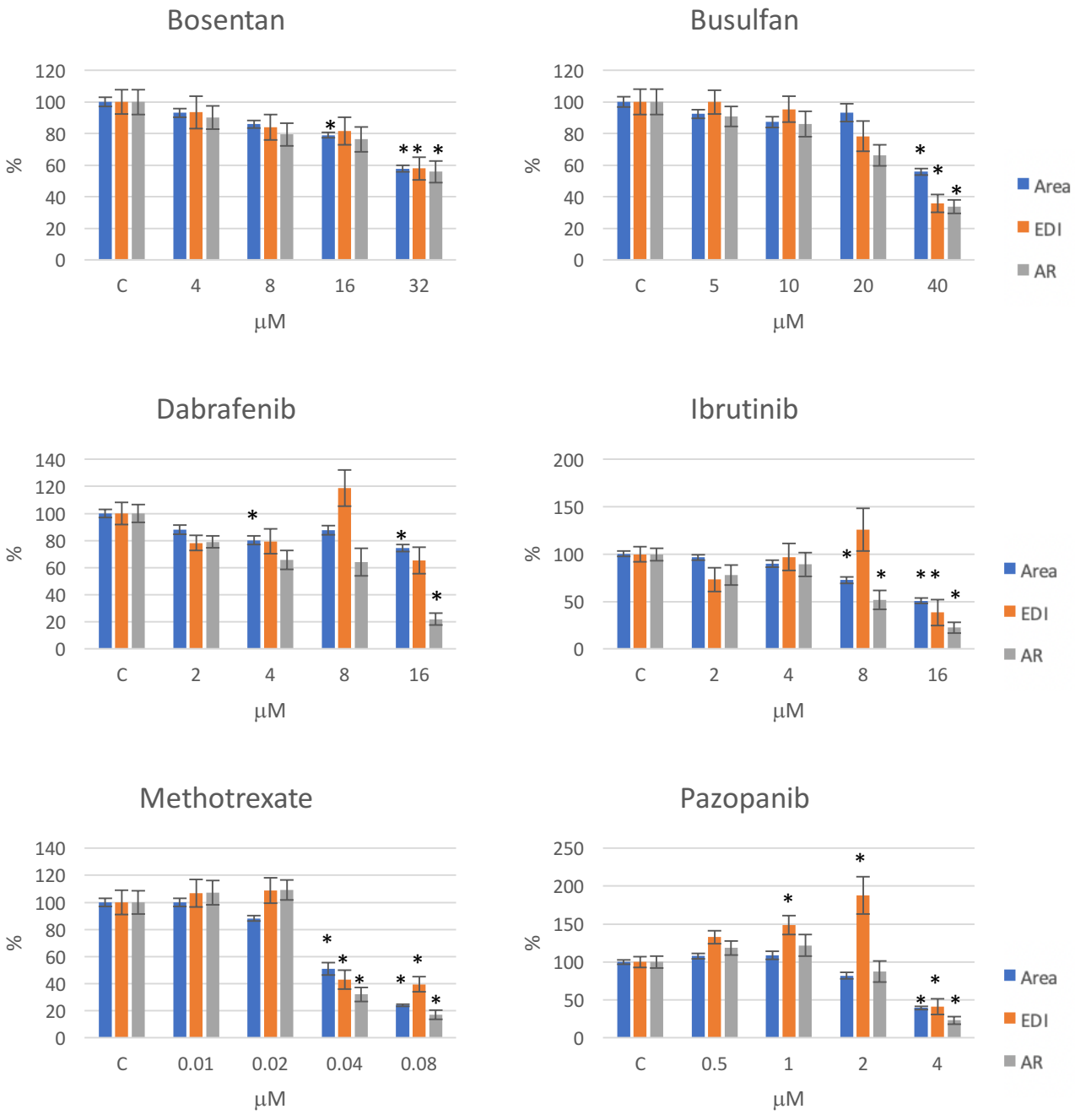
Bosentan
120
100
80
60
40
20
0
%
C
4
8
16
32
μM
Busulfan
120
100
80
60
40
20
0
%
C
5
10
20
40
μM
Area
EDI
AR
Dabrafenib
140
120
100
80
60
40
20
0
%
C
2
4
8
16
μM
Ibrutinib
200
150
100
50
0
%
C
2
4
8
16
μM
Area
EDI
AR
Methotrexate
140
120
100
80
60
40
20
0
%
C
0.01
0.02
0.04
0.08
μM
Pazopanib
250
200
150
100
50
0
%
C
0.5
1
2
4
μM
Area
EDI
AR

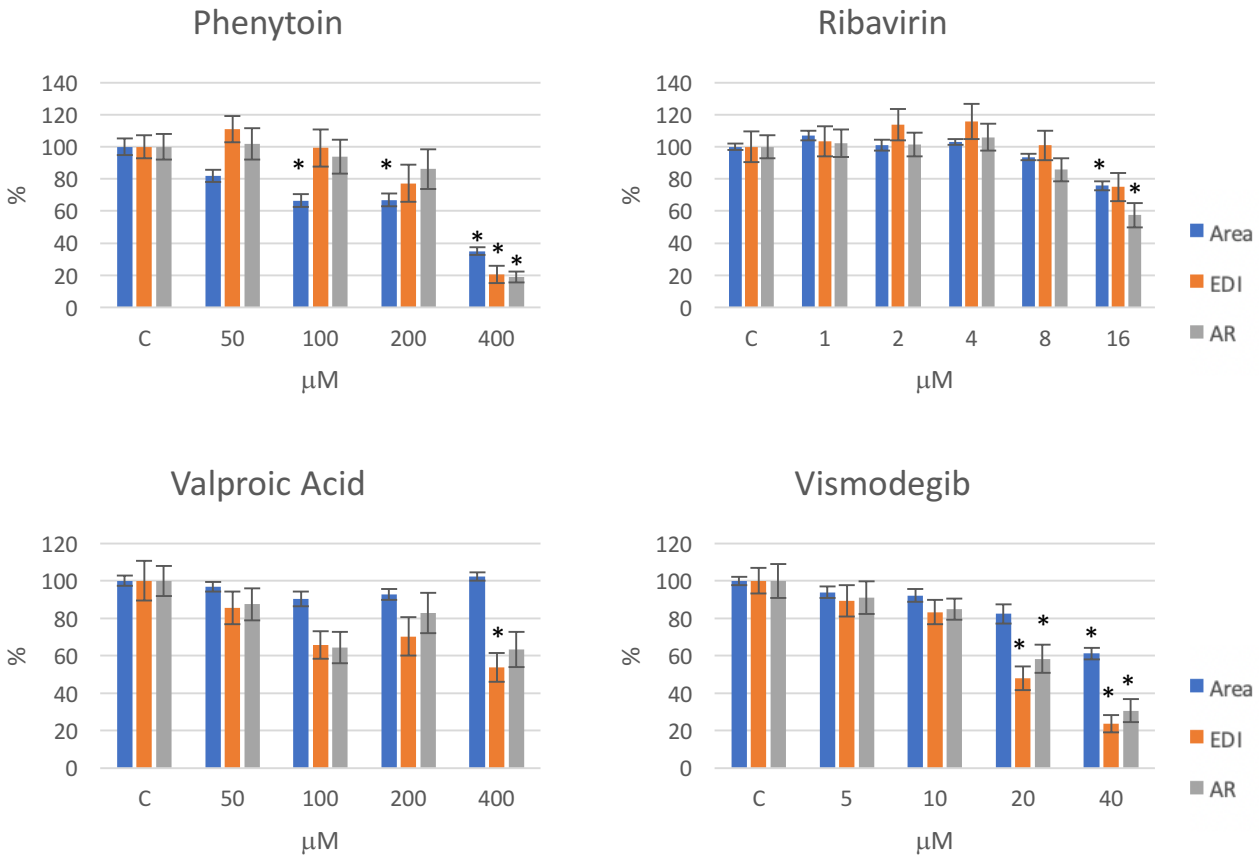

Figure 1: Impact of various teratogens on P19C5 EB morphology. EBs were treated with varying concentrations (μM) of 10 different known teratogens and morphology was analyzed on day 4 of culture. Graph shows relative area (blue column), relative EDI (orange column), relative AR (grey column). Error bars represent 95% confidence interval and stars represent significant differences from control (p-value <0.01) that meet the adverse effect criteria: a reduction in area by >20% and/or a change in shape (EDI or AR) by >40%.

A

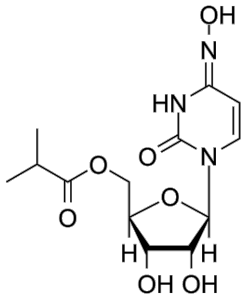

Molnupiravir (EIDD-2801)

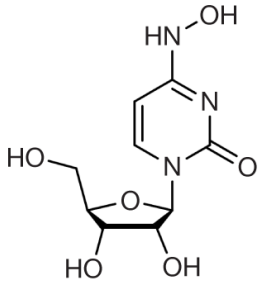

N-hydroxycytidine (NHC, EIDD-1931)

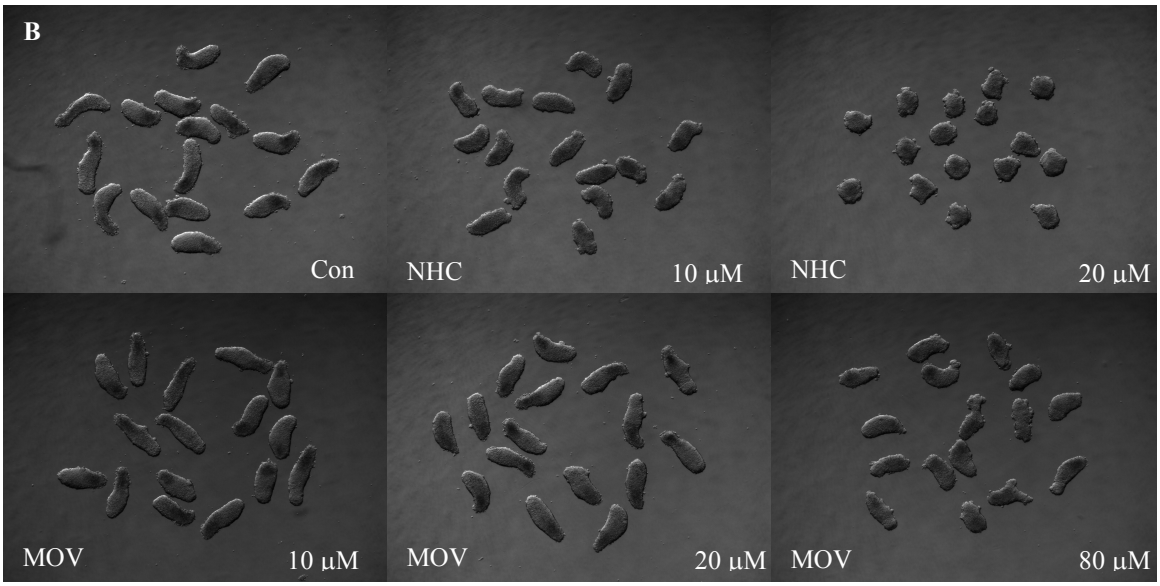

C

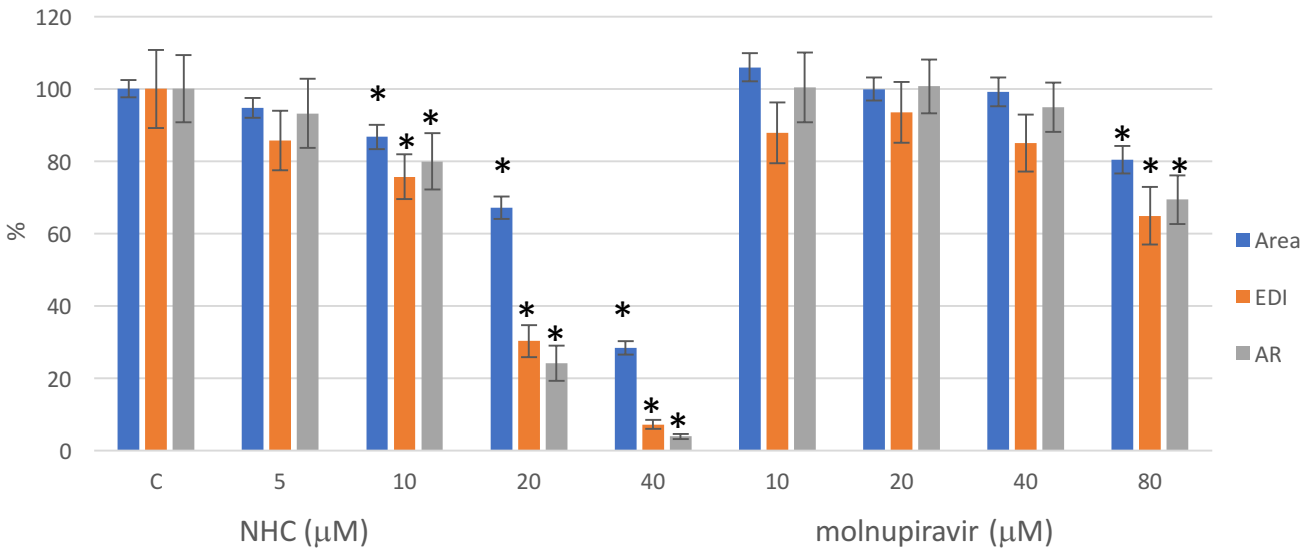

Figure 2: Impact of molnupiravir and NHC on P19C5 EB morphology. EBs were treated with 10-80 μM of molnupiravir or 5-40 μM of NHC and morphology was analyzed on day 4 of culture. **A.** Chemical structure of molnupiravir and NHC. **B.** Images of EBs at day 4 of culture after being treated with varying concentrations of molnupiravir (MOV) or NHC compared to control. **C.** Graph shows relative area (blue column), relative EDI (orange column), relative AR (grey column). Error bars represent 95% confidence interval and stars represent significant differences from control (p-value <0.01) with more than 10% reduction.

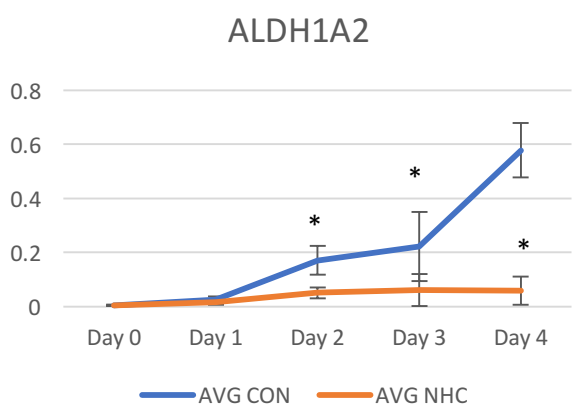
ALDH1A2
0.8
0.6
0.4
0.2
0
Day 0
Day 1
Day 2
Day 3
Day 4
AVG CON
AVG NHC

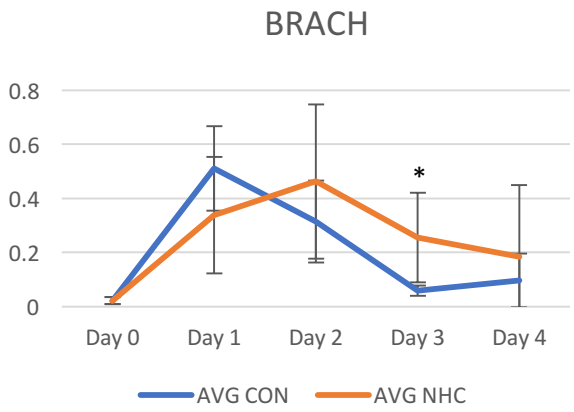
BRACH
0.8
0.6
0.4
0.2
0
Day 0
Day 1
Day 2
Day 3
Day 4
AVG CON
AVG NHC

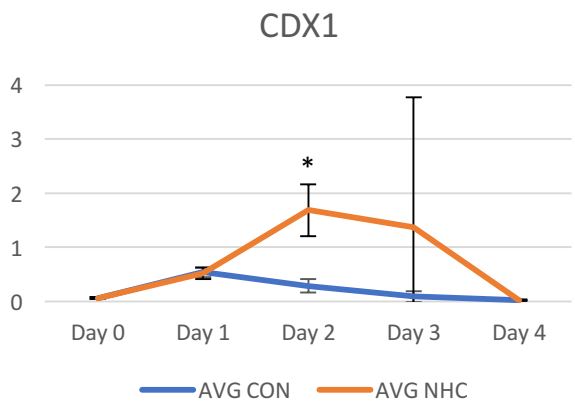
CDX1
4
3
2
1
0
Day 0
Day 1
Day 2
Day 3
Day 4
AVG CON
AVG NHC

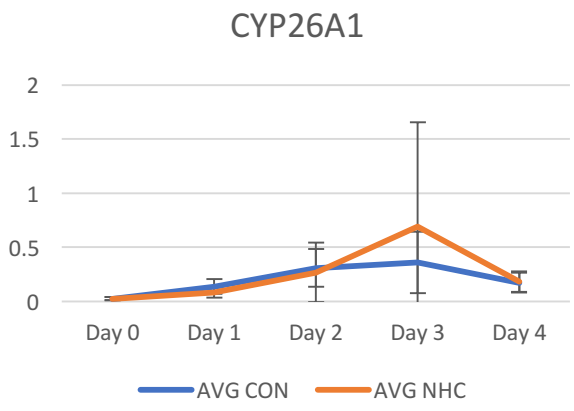
CYP26A1
2
1.5
1
0.5
0
Day 0
Day 1
Day 2
Day 3
Day 4
AVG CON
AVG NHC

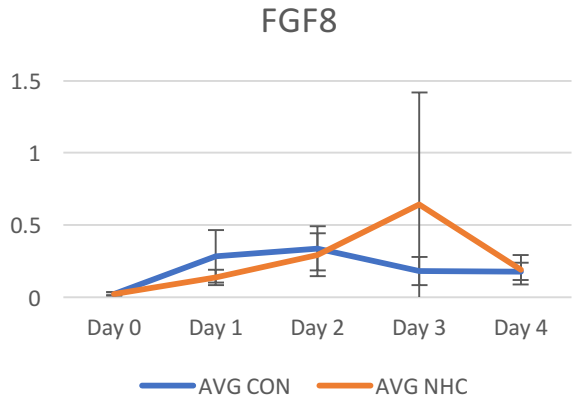
FGF8
1.5
1
0.5
0
Day 0
Day 1
Day 2
Day 3
Day 4
AVG CON
AVG NHC

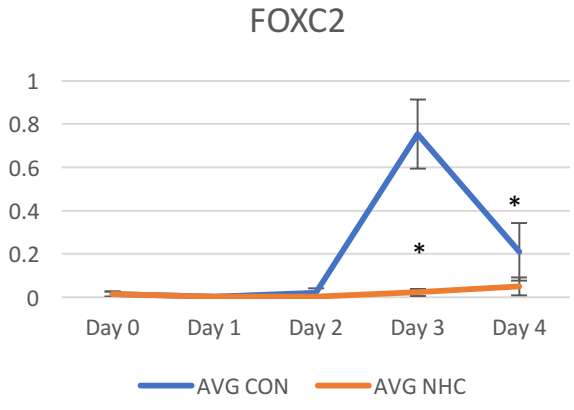
FOXC2
1
0.8
0.6
0.4
0.2
0
Day 0
Day 1
Day 2
Day 3
Day 4
AVG CON
AVG NHC

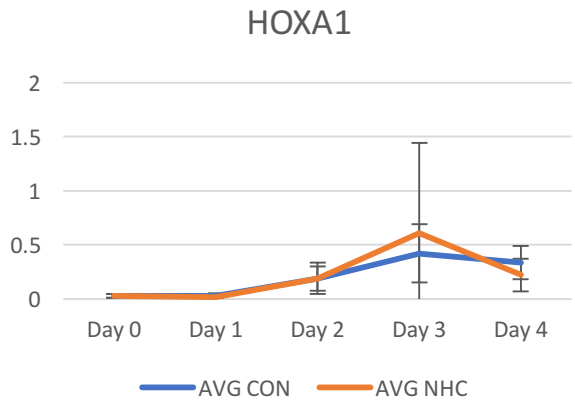
HOXA1
2
1.5
1
0.5
0
Day 0
Day 1
Day 2
Day 3
Day 4
AVG CON
AVG NHC

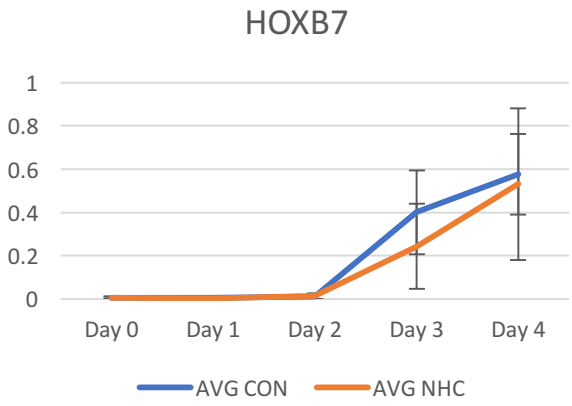
HOXB7
1
0.8
0.6
0.4
0.2
0
Day 0
Day 1
Day 2
Day 3
Day 4
AVG CON
AVG NHC

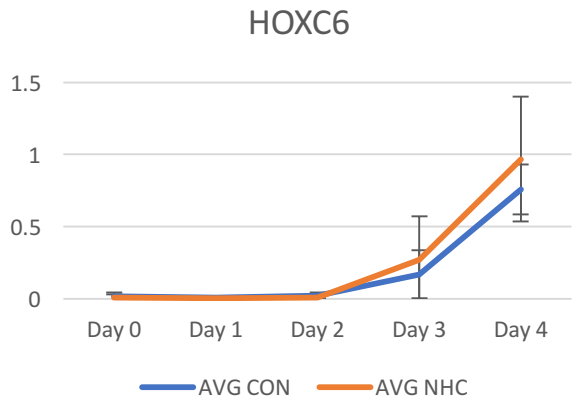
HOXC6
1.5
1
0.5
0
Day 0
Day 1
Day 2
Day 3
Day 4
AVG CON
AVG NHC

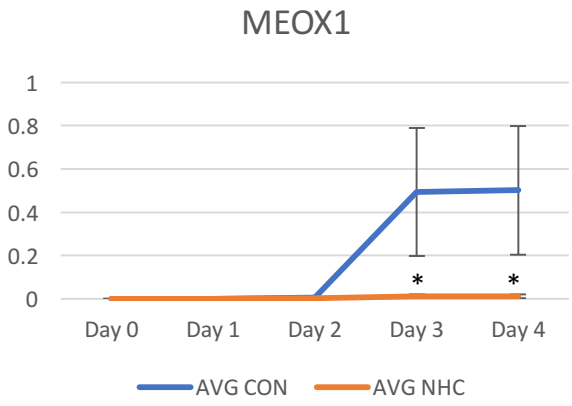
MEOX1
1
0.8
0.6
0.4
0.2
0
*
*
Day 0
Day 1
Day 2
Day 3
Day 4
AVG CON
AVG NHC

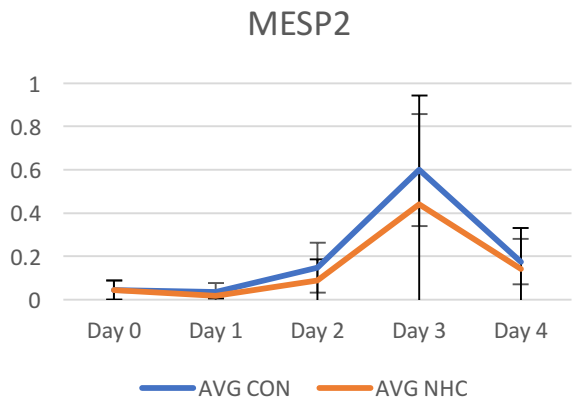
MESP2
1
0.8
0.6
0.4
0.2
0
Day 0
Day 1
Day 2
Day 3
Day 4
AVG CON
AVG NHC

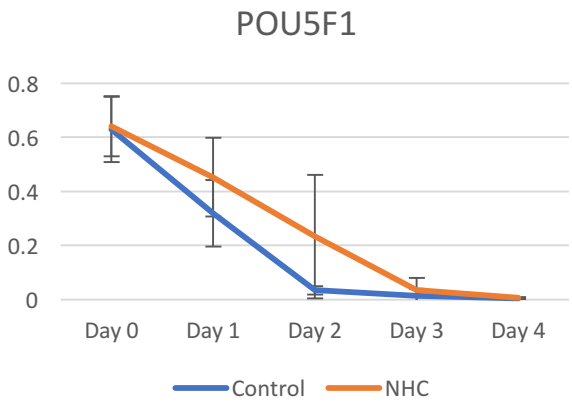
POU5F1
0.8
0.6
0.4
0.2
0
Day 0
Day 1
Day 2
Day 3
Day 4
Control
NHC

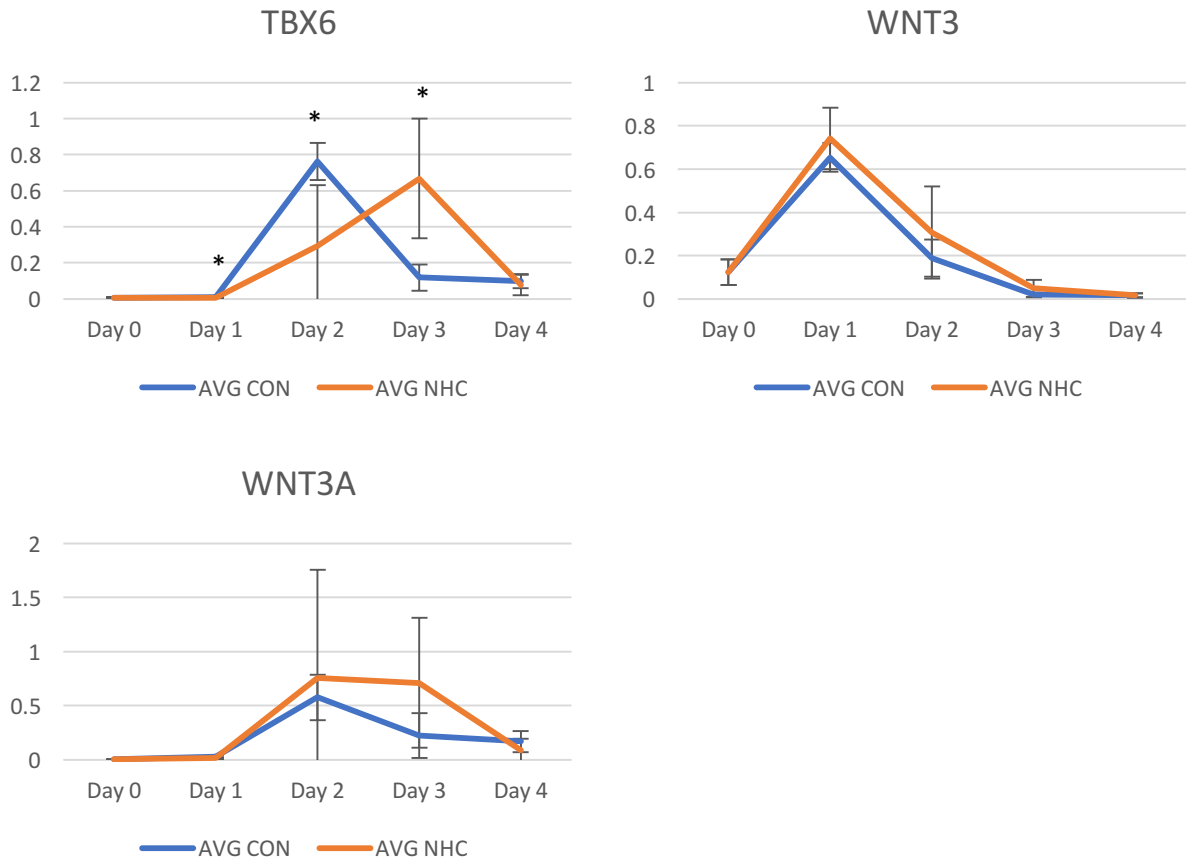

Figure 3: Expression of developmental regulators in NHC exposed P19C5 EBs. EBs were treated with 20 μM of NHC and gene expression patterns were analyzed on each day of culture for 4 days. Graphs show the expression of different developmental regulator genes over 4 days of culture in control (blue line) and NHC-treated (Orange line) EBs. Error bars represent standard deviation and stars represent significant change from control (p value < 0.05).

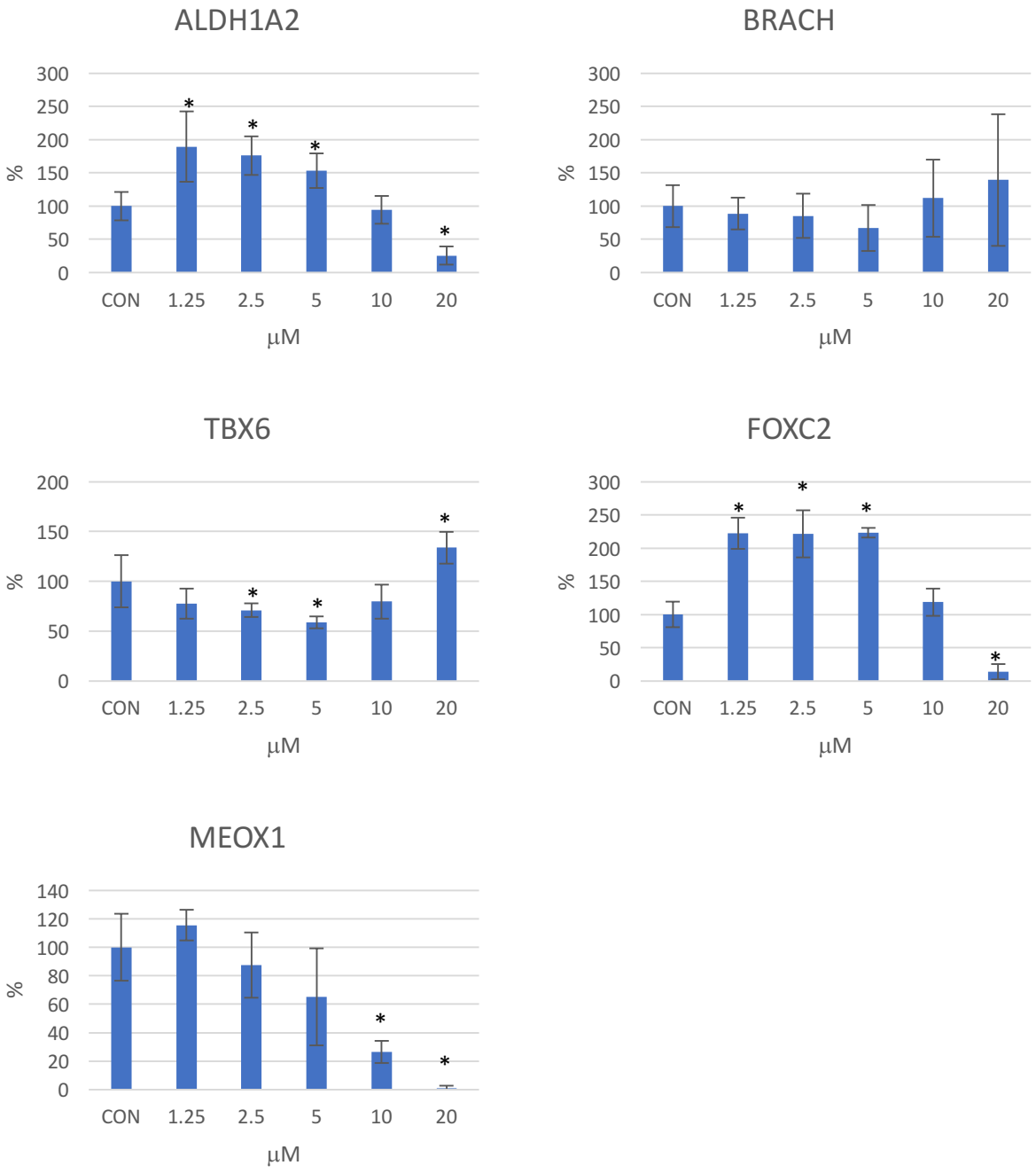

Figure 4: Expression of developmental regulators in NHC-exposed P19C5 EBs at Day 3. EBs were treated with 1.25- 20 µM of NHC and expression patterns were analyzed on day 3 of culture. Graphs show expression of different developmental regulator genes at different concentrations of NHC at day 3 of culture. Error bars represent standard deviation and stars represent significant difference from control (p-value < 0.05).

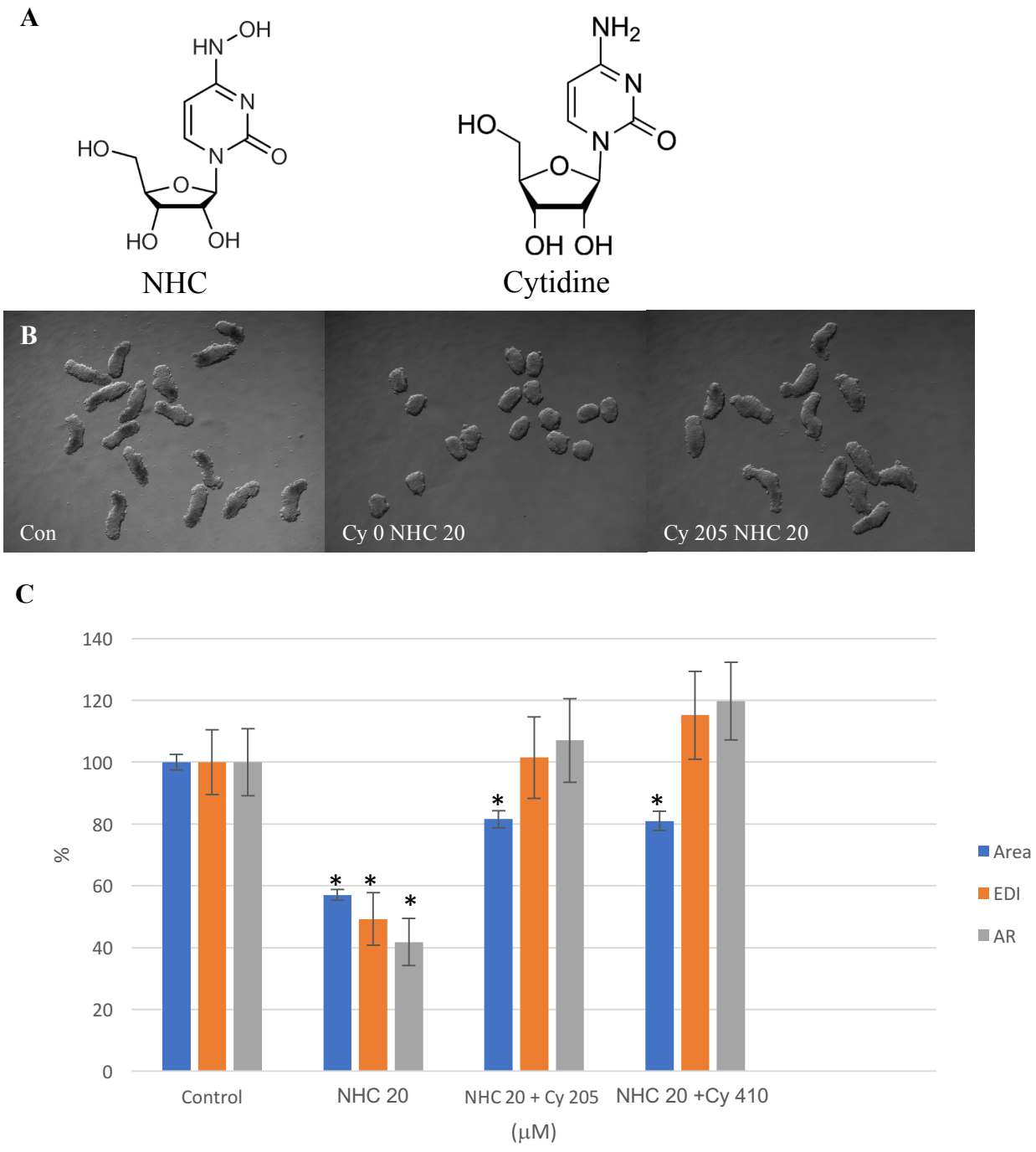

Figure 5: Impact of excess exposure of cytidine on morphology in NHC-treated EBs. EBs were treated with 20 μM of NHC with or without 205-410 μM of cytidine nucleoside (Cy) and morphology was analyzed on day 4 of culture. **A.** Chemical structure of NHC and Cytidine. **B.** Images of EBs at day 4 of culture after being treated with varying concentrations of cytidine and/or NHC compared to control. **C.** Graph shows relative area (blue column), relative EDI (orange column), relative AR (grey column). Error bars represent 95% confidence interval and stars represent significant differences from control (p-value <0.01).

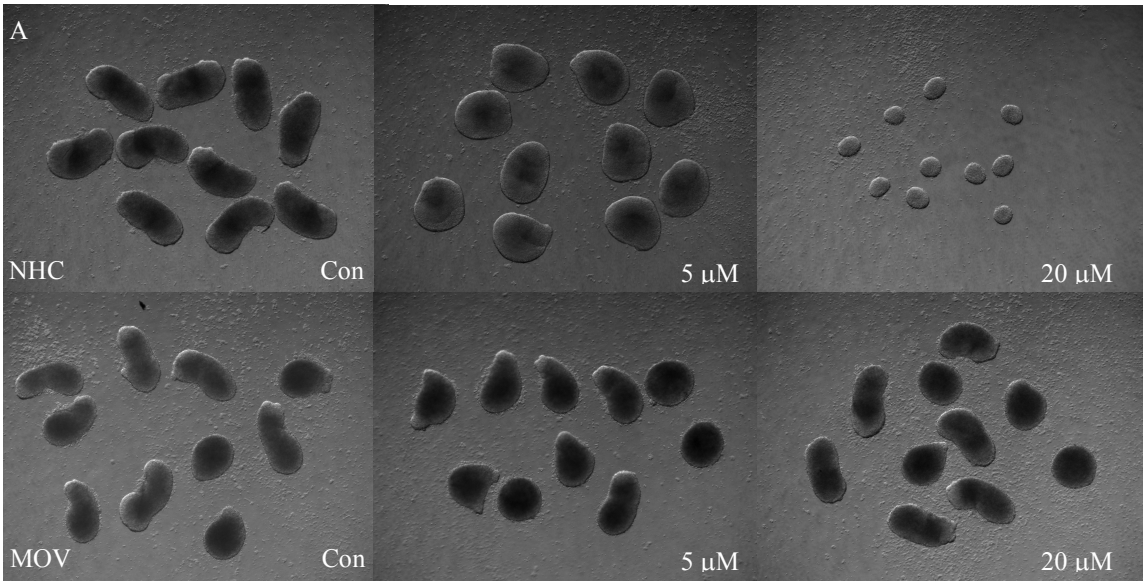

B

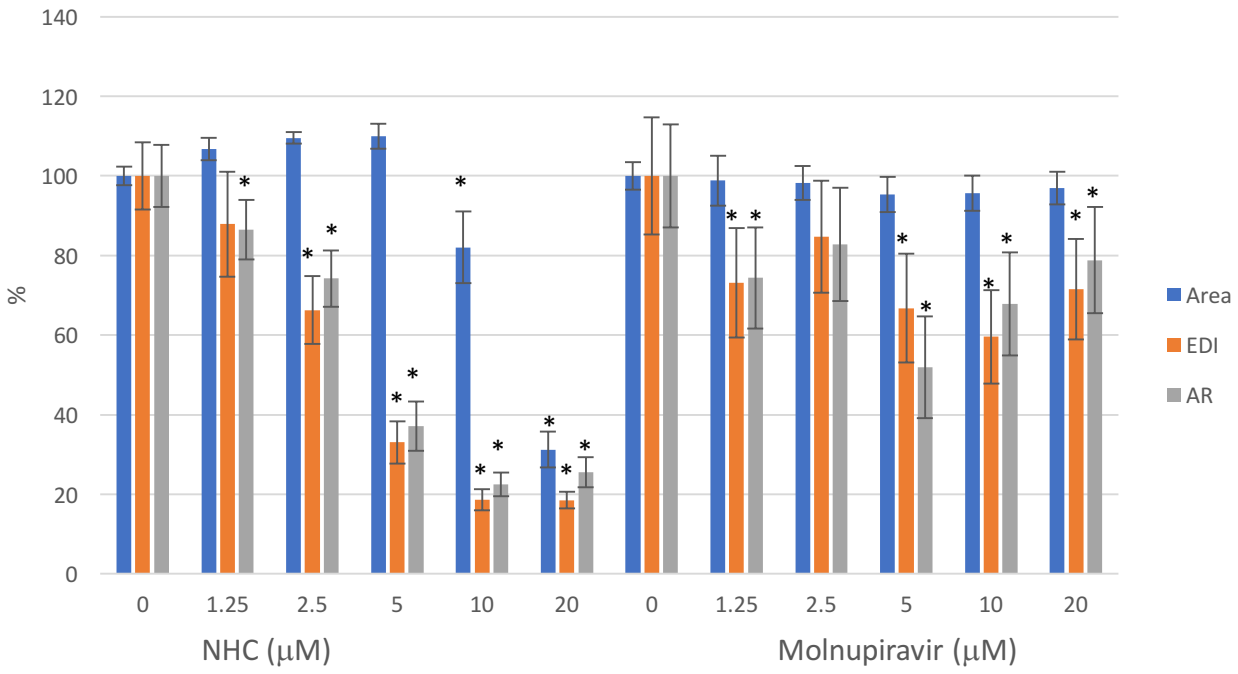

Figure 6: Impact of molnupiravir and NHC on human EB morphology. EBs were treated with 1.25-20 µM of molnupiravir or NHC and morphology was analyzed on day 4 of culture. **A.** Images of EBs at day 4 of culture after being treated with varying concentrations of molnupiravir (MOV) or NHC compared to control. **B.** Graph shows relative area (blue column), relative EDI (orange column), relative AR (grey column). Error bars represent 95% confidence interval and stars represent significant differences from control (p-value <0.01) with more than 10% reduction.

Bibliography

Amara, A., Penchala, S. D., Else, L., Hale, C., FitzGerald, R., Walker, L., Lyons, R., Fletcher, T., & Khoo, S. (2021). The development and validation of a novel LC-MS/MS method for the simultaneous quantification of Molnupiravir and its metabolite ß-d-N4-hydroxycytidine in human plasma and saliva. *Journal of Pharmaceutical and Biomedical Analysis*, *206*, 114356. https://doi.org/10.1016/j.jpba.2021.114356

Beta-d-N4-Hydroxycytidine. (n.d.). Cell Signaling Technology. Retrieved April 19, 2023, from https://www.cellsignal.com/products/activators-inhibitors/beta-d-n4-hydroxycytidine/81178

Blanchard, K. (2021, November 30). *Molnupiravir*. Antimicrobial Drugs Advisory Committee. https://www.fda.gov/media/154472/download

Cohen, J. & Piller, C. (2020, May 13). *Emails offer look into whistleblower charges of cronyism behind potential COVID-19 drug*. Science. Retrieved February 23, 2023, from https://www.science.org/content/article/emails-offer-look-whistleblower-charges-cronyism-behind-potential-covid-19-drug

Cox, R. M., Wolf, J. D., & Plemper, R. K. (2021). Therapeutically administered ribonucleoside analogue MK-4482/EIDD-2801 blocks SARS-CoV-2 transmission in ferrets. *Nature Microbiology*, *6*(1), 11-18. https://doi.org/10.1038/s41564-020-00835-2

Cytidine (Cytosine β-D-riboside) | Nucleoside Molecule | MedChemExpress. (n.d.). MedchemExpress.Com. Retrieved April 19, 2023, from https://www.medchemexpress.com/Cytidine.html

DeSesso, J. M., & Scialli, A. R. (2018). Bone development in laboratory mammals used in developmental toxicity studies. *Birth Defects Research*, *110*(15), 1157–1187. https://doi.org/10.1002/bdr2.1350

Drugs.com, FDA Pregnancy Categories Explained. Retrieved March 11, 2023, from https://www.drugs.com/pregnancy-categories.html

Ehteshami, M., Tao, S., Zandi, K., Hsiao, H.-M., Jiang, Y., Hammond, E., Amblard, F., Russell, O. O., Merits, A., & Schinazi, R. F. (2017). Characterization of β-d-N4-Hydroxycytidine as a Novel Inhibitor of Chikungunya Virus. *Antimicrobial Agents and Chemotherapy*, *61*(4), e02395-16. https://doi.org/10.1128/AAC.02395-16

European Medicines Agency. (2020). ICH S5 (R3) guideline on reproductive toxicology: Detection of Toxicity to Reproduction for Human Pharmaceuticals. https://www.ema.europa.eu/en/ich-s5-r3-guideline-reproductive-toxicology-detection-toxicity-reproduction-human-pharmaceuticals

EMA. (2021, October 25). *COVID-19: EMA starts rolling review of molnupiravir* [Text]. European Medicines Agency. https://www.ema.europa.eu/en/news/covid-19-ema-starts-rolling-review-molnupiravir

EMA. (2021, November 19). *EMA issues advice on use of Lagevrio (molnupiravir) for the treatment COVID-19* [Text]. European Medicines Agency. https://www.ema.europa.eu/en/news/ema-issues-advice-use-lagevrio-molnupiravir-treatment-covid-19

Emergency Use Authorization Declaration. (2020, April 1). Federal Register. https://www.federalregister.gov/documents/2020/04/01/2020-06905/emergency-use-authorization-declaration

FDA. (2018). *The Drug Development Process*. FDA; FDA. https://www.fda.gov/patients/learn-about-drug-and-device-approvals/drug-development-process

FDA. (2023). Emergency Use Authorization. *FDA*. https://www.fda.gov/emergency-preparedness-and-response/mcm-legal-regulatory-and-policy-framework/emergency-use-authorization

Fischerii, W. A., Eron Jr., J. J., Holman, W., Cohen, M. S., Fang, L., Szewczyk, L. J., Sheahan, T. P., Baric, R. S., Mollan, K. R., & Painter, W. P. (2021). A phase 2a clinical trial of molnupiravir in patients with COVID-19 shows accelerated SARS-CoV-2 RNA clearance and elimination of infectious virus | Science Translational Medicine. *Science Translational Medicine*, *14*(628). https://doi.org/10.1126/scitranslmed.abl7430

Garcia, G., Sharma, A., Ramaiah, A., Sen, C., Purkayastha, A., Kohn, D. B., Parcells, M. S., Beck, S., Kim, H., Bakowski, M. A., Kirkpatrick, M. G., Riva, L., Wolff, K. C., Han, B., Yuen, C., Ulmert, D., Purbey, P. K., Scumpia, P., Beutler, N., … Arumugaswami, V. (2021). Antiviral drug screen identifies DNA-damage response inhibitor as potent blocker of SARS-CoV-2 replication. *Cell Reports*, *35*(1), 108940. https://doi.org/10.1016/j.celrep.2021.108940

Gouti, M., Delile, J., Stamataki, D., Wymeersch, F. J., Huang, Y., Kleinjung, J., Wilson, V., & Briscoe, J. (2017). A Gene Regulatory Network Balances Neural and Mesoderm Specification during Vertebrate Trunk Development. *Developmental Cell*, *41*(3), 243-261.e7. https://doi.org/10.1016/j.devcel.2017.04.002

Guo, X., Yi, H., Li, T. C., Wang, Y., Wang, H., & Chen, X. (2021). Role of Vascular Endothelial Growth Factor (VEGF) in Human Embryo Implantation: Clinical Implications. *Biomolecules*, *11*(2), 253. https://doi.org/10.3390/biom11020253

Gupta, M., & Tripp, J. (2023). Phenytoin. In *StatPearls*. StatPearls Publishing. http://www.ncbi.nlm.nih.gov/books/NBK551520/

Halford, B. (2020, May 5). An emerging antiviral takes aim at COVID-19. *Chemical and Engineering News*. https://cen.acs.org/pharmaceuticals/drug-development/emerging-antiviral-takes-aim-COVID-19/98/web/2020/05

Hannoodee, M., & Mittal, M. (2023). Methotrexate. In *StatPearls*. StatPearls Publishing. http://www.ncbi.nlm.nih.gov/books/NBK556114/

Hashemian, S. M. R., Pourhanifeh, M. H., Hamblin, M. R., Shahrzad, M. K., & Mirzaei, H. (2022). RdRp inhibitors and COVID-19: Is molnupiravir a good option? *Biomedicine & Pharmacotherapy*, *146*, 112517. https://doi.org/10.1016/j.biopha.2021.112517

Hernandez-Santiago, B. I., Beltran, T., Stuyver, L., Chu, C. K., & Schinazi, R. F. (2004). Metabolism of the anti-hepatitis C virus nucleoside beta-D-N4-hydroxycytidine in different liver cells. *Antimicrobial Agents and Chemotherapy*, *48*(12), 4636–4642. https://doi.org/10.1128/AAC.48.12.4636-4642.2004

Hu, W., Chang, L., Yang, Y., Wang, X., Xie, Y., Shen, J., Tan, B., & Liu, J. (2021). Pharmacokinetics and tissue distribution of remdesivir and its metabolites nucleotide monophosphate, nucleotide triphosphate, and nucleoside in mice. *Acta Pharmacologica Sinica*, *42*(7), Article 7. https://doi.org/10.1038/s41401-020-00537-9

Hughes, Mike, & Health, J. B. S. of P. (n.d.). *The Principles of Humane Experimental Technique: Chapter 4*. Johns Hopkins Bloomberg School of Public Health. Retrieved April 10, 2023, from http://caat.jhsph.edu/principles/chap4d

Kabinger, F., Stiller, C., Schmitzová, J., Dienemann, C., Kokic, G., Hillen, H. S., Höbartner, C., & Cramer, P. (2021). Mechanism of molnupiravir-induced SARS-CoV-2 mutagenesis. *Nature Structural & Molecular Biology*, *28*(9), Article 9. https://doi.org/10.1038/s41594-021-00651-0

Kearl, Megan, Dickey-Wicker Amendment, 1996. *Embryo Project Encyclopedia* (2010-08-27). ISSN: 1940-5030 http://embryo.asu.edu/handle/10776/2050.

Lau, C. G. & Marikawa, Y. (2014). Morphology-based mammalian stem cell tests reveal potential developmental toxicity of donepezil. *Mol. Repro. Dev. 81,* 994-1008.

Li, A.S. & Marikawa, Y. (2015). An in vitro gastrulation model recapitulates the morphogenetic impact of pharmacological inhibitors of developmental signaling pathways. *Mol. Repro. Dev* 82, 1015-1036.

Li, A.S. & Marikawa, Y. (2016). Adverse effect of valproic acid on an in vitro gastrulation model entails activation of retinoic acid signaling. *Reprod. Toxicol* 66, 68-83.

Liu, Q., Gupta, A., Okesli-Armlovich, A., Qiao, W., Fischer, C. R., Smith, M., Carette, J. E., Bassik, M. C., & Khosla, C. (2020). Enhancing the Antiviral Efficacy of RNA-Dependent RNA Polymerase Inhibition by Combination with Modulators of Pyrimidine Metabolism. *Cell Chemical Biology*, *27*(6), 668-677.e9. https://doi.org/10.1016/j.chembiol.2020.05.002

Lo, B., & Parham, L. (2009). Ethical Issues in Stem Cell Research. *Endocrine Reviews*, *30*(3), 204–213. https://doi.org/10.1210/er.2008-0031

Malone, B., & Campbell, E. A. (2021). Molnupiravir: Coding for catastrophe. *Nature Structural & Molecular Biology*, *28*(9), Article 9. https://doi.org/10.1038/s41594-021-00657-8

Mankoo, B. S., Skuntz, S., Harrigan, I., Grigorieva, E., Candia, A., Wright, C. V. E., Arnheiter, H., & Pachnis, V. (2003). The concerted action of Meox homeobox genes is required upstream of genetic pathways essential for the formation, patterning and differentiation of somites. *Development (Cambridge, England)*, *130*(19), 4655–4664. https://doi.org/10.1242/dev.00687

Marikawa, Y., Tamashiro, D. A., Fujita, T. C., Alarcon, V. B. (2009). Aggregated P19 mouse embryonal carcinoma cells as a simple in vitro model to study the molecular regulations of mesoderm formation and axial elongation morphogenesis, *Genesis, 47*, 93-106.

Marikawa, Y., Chen, H., Menor, M., Deng, Y., Alarcon, V. B. (2020). Exposure-based assessment of chemical teratogenicity using morphogenetic aggregates of human embryonic stem cells. *Reproductive Toxicity* 91, 74-91. https://doi.org/10.1016/j.reprotox.2019.10.004

Masarweh, O. M., & Bhardwaj, A. (2023). Bosentan. In *StatPearls*. StatPearls Publishing. http://www.ncbi.nlm.nih.gov/books/NBK542293/

Merck. (2023). *Fact sheet for healthcare providers: emergency use authorization for lagevrio (molnupiravir) capsules.* https://www.merck.com/eua/molnupiravir-hcp-fact-sheet.pdf

Molnupiravir: Uses, Interactions, Mechanism of Action | DrugBank Online. (n.d.). Retrieved November 21, 2022, from https://go.drugbank.com/drugs/DB15661

Moon, A. M. (2006). Mouse Models for Investigating the Developmental Basis of Human Birth Defects. *Pediatric Research*, *59*(6), Article 6. https://doi.org/10.1203/01.pdr.0000218420.00525.98

National Center for Biotechnology Information (2023). PubChem Compound Summary for CID 44462760, Dabrafenib. Retrieved April 20, 2023 from https://pubchem.ncbi.nlm.nih.gov/compound/Dabrafenib.

National Center for Biotechnology Information (2023). PubChem Compound Summary for CID 24821094, Ibrutinib. Retrieved April 20, 2023 from https://pubchem.ncbi.nlm.nih.gov/compound/Ibrutinib.

National Center for Biotechnology Information (2023). PubChem Compound Summary for CID 197020, N(4)-Hydroxycytidine. Retrieved April 20, 2023 from https://pubchem.ncbi.nlm.nih.gov/compound/N_4_-Hydroxycytidine.

National Center for Biotechnology Information (2023). PubChem Compound Summary for CID 10113978, Pazopanib. Retrieved April 20, 2023 from https://pubchem.ncbi.nlm.nih.gov/compound/Pazopanib.

National Center for Biotechnology Information (2023). PubChem Compound Summary for CID 37542, Ribavirin. Retrieved April 20, 2023 from https://pubchem.ncbi.nlm.nih.gov/compound/Ribavirin.

Niederreither, K., Subbarayan, V., Dollé, P., & Chambon, P. (1999). Embryonic retinoic acid synthesis is essential for early mouse post-implantation development. *Nature Genetics*, *21*(4), 444–448. https://doi.org/10.1038/7788

Ornoy, A. (2009). Valproic acid in pregnancy: How much are we endangering the embryo and fetus? *Reproductive Toxicology (Elmsford, N.Y.)*, *28*(1), 1–10. https://doi.org/10.1016/j.reprotox.2009.02.014

Painter, W.P. (2020). *Overview of EIDD-2801 (MK-4482).* Special isirv-AVG Virtual Conference on 'Therapeutics for COVID-19'. https://mod.isirv.org/repository/avg_2020/Wendy_Painter.pdf

Painter, W. P., Holman, W., Bush, J. A., Almazedi, F., Malik, H., Eraut, N. C. J. E., Morin, M. J., Szewczyk, L. J., & Painter, G. R. (2021). Human Safety, Tolerability, and Pharmacokinetics of Molnupiravir, a Novel Broad-Spectrum Oral Antiviral Agent with Activity against SARS-CoV-2. *Antimicrobial Agents and Chemotherapy*, *65*(5), e02428-20. https://doi.org/10.1128/AAC.02428-20

Patel, R., & Tadi, P. (2023). Busulfan. In *StatPearls*. StatPearls Publishing. http://www.ncbi.nlm.nih.gov/books/NBK555986/

Sarayani, A., Albogami, Y., Thai, T. N., Smolinski, N. E., Patel, P., Wang, Y., Nduaguba, S., Rasmussen, S. A., & Winterstein, A. G. (2022). Prenatal exposure to teratogenic medications in the era of Risk Evaluation and Mitigation Strategies. *American Journal of Obstetrics & Gynecology*, *227*(2), 263.e1-263.e38. https://doi.org/10.1016/j.ajog.2022.01.004

Sheahan, T. P., Sims, A. C., Zhou, S., Graham, R. L., Pruijssers, A. J., Agostini, M. L., Leist, S. R., Schäfer, A., Dinnon, K. H., Stevens, L. J., Chappell, J. D., Lu, X., Hughes, T. M., George, A. S., Hill, C. S., Montgomery, S. A., Brown, A. J., Bluemling, G. R., Natchus, M. G., … Baric, R. S. (2020). An orally bioavailable broad-spectrum antiviral inhibits SARS-CoV-2 in human airway epithelial cell cultures and multiple coronaviruses in mice. *Science Translational Medicine*, eabb5883. https://doi.org/10.1126/scitranslmed.abb5883

Singh, A. K., Singh, A., Singh, R., & Misra, A. (2021). Molnupiravir in COVID-19: A systematic review of literature. *Diabetes & Metabolic Syndrome*, *15*(6), 102329. https://doi.org/10.1016/j.dsx.2021.102329

Sticher, Z. M., Lu, G., Mitchell, D. G., Marlow, J., Moellering, L., Bluemling, G. R., Guthrie, D. B., Natchus, M. G., Painter, G. R., & Kolykhalov, A. A. (2020a). Analysis of the Potential for N4-Hydroxycytidine To Inhibit Mitochondrial Replication and Function. *Antimicrobial Agents and Chemotherapy*, *64*(2), e01719-19. https://doi.org/10.1128/AAC.01719-19

Tantibanchachai, Chanapa, "Teratogens". *Embryo Project Encyclopedia* (2014-01-22). ISSN: 1940-5030 http://embryo.asu.edu/handle/10776/7510.

National Institute of Child Health and Human Development (NICHD). *Task Force on Research Specific to Pregnant Women and Lactating Women (PRGLAC)*. (2022, October 20). https://www.nichd.nih.gov/about/advisory/PRGLAC

Troth, S., Butterton, J., DeAnda, C. S., Escobar, P., Grobler, J., Hazuda, D., & Painter, G. (2021). Letter to the Editor in Response to Zhou et al. *The Journal of Infectious Diseases*, *224*(8), 1442–1443. https://doi.org/10.1093/infdis/jiab362

Urakova, N., Kuznetzova, V., Crossman, D. K., Sokratian, R., Guthrie, D. B., Kolykhalov, A. A., Lockwood, M. A., Natchus, M. G., Crowley, M. R., Painter, G. R., Frolova, E. I. (2018). β-d-N4-Hydroxycytidine Is a Potent Anti-alphavirus Compound That Induces a High Level of Mutations in the Viral Genome | *Journal of Virology*. 29(3), e01965-17. https://doi.org/10.1128/JVI.01965-17.

Vargesson, N. (2015). Thalidomide-induced teratogenesis: History and mechanisms. *Birth Defects Research*, *105*(2), 140–156. https://doi.org/10.1002/bdrc.21096

Wadman, M. (2023, January, 10). *FDA no longer needs to require animal tests before human drug trials*. Science. Retrieved February 22, 2023, from https://www.science.org/content/article/fda-no-longer-needs-require-animal-tests-human-drug-trials

Wahl, A., Gralinski, L. E., Johnson, C. E., Yao, W., Kovarova, M., Dinnon, K. H., Liu, H., Madden, V. J., Krzystek, H. M., De, C., White, K. K., Gully, K., Schäfer, A., Zaman, T., Leist, S. R., Grant, P. O., Bluemling, G. R., Kolykhalov, A. A., Natchus, M. G., … Garcia, J. V. (2021). SARS-CoV-2 Infection is Effectively Treated and Prevented by EIDD-2801. *Nature*, *591*(7850), 451–457. https://doi.org/10.1038/s41586-021-03312-w

Warkus, E. L. L. & Marikawa, Y. (2017). Exposure-based validation of an in vitro gastrulation model for developmental toxicity assays. *Toxicol. Sci.* 157, 235-245.

Warkus, E. L. L. & Marikawa, Y. (2018). Fluoxetine inhbits canonaical Wnt signaling to impair embryoid body morphogenesis: potential teratogenic mechanisms of a commonly used antidepressant. *Toxilogical Sciences,* 165(2), 372-388. https://doi.10.1093/toxsci/kfy143

Waters, M. D., Warren, S., Hughes, C., Lewis, P., & Zhang, F. (2022). Human genetic risk of treatment with antiviral nucleoside analog drugs that induce lethal mutagenesis: The special case of molnupiravir. *Environmental and Molecular Mutagenesis*, *63*(1), 37–63. https://doi.org/10.1002/em.22471

Wen, W., Chen, C., Tang, J., Wang, C., Zhou, M., Cheng, Y., Zhou, X., Wu, Q., Zhang, X., Feng, Z., Wang, M., & Mao, Q. (2022). Efficacy and safety of three new oral antiviral treatment (molnupiravir, fluvoxamine and Paxlovid) for COVID-19：a meta-analysis. *Annals of Medicine*, *54*(1), 516–523. https://doi.org/10.1080/07853890.2022.2034936

Winnier, G. E., Hargett, L., & Hogan, B. L. M. (1997). The winged helix transcription factor MFHl is required for proliferation and patterning of paraxial mesoderm in the mouse embryo. *Gene Dev 11*(9), 926-940. https://doi.org/10.1101/gad.11.7.926

Zhou, S., Hill, C. S., Sarkar, S., Tse, L. V., Woodburn, B. M. D., Schinazi, R. F., Sheahan, T. P., Baric, R. S., Heise, M. T., & Swanstrom, R. (2021). β-d-N4-hydroxycytidine Inhibits SARS-CoV-2 Through Lethal Mutagenesis But Is Also Mutagenic To Mammalian Cells. *The Journal of Infectious Diseases*, *224*(3), 415–419. https://doi.org/10.1093/infdis/jiab247

Zito, P. M., Nassereddin, A., & Scharf, R. (2023). Vismodegib. In *StatPearls*. StatPearls Publishing. http://www.ncbi.nlm.nih.gov/books/NBK513360/